Integrating alternative fuels in a patrol vessel fleet

Adopting alternative climate neutral energy carriers to contribute to an environmentally friendly future

Thesis Report

Loet van den Elsen

Delft University of Technology

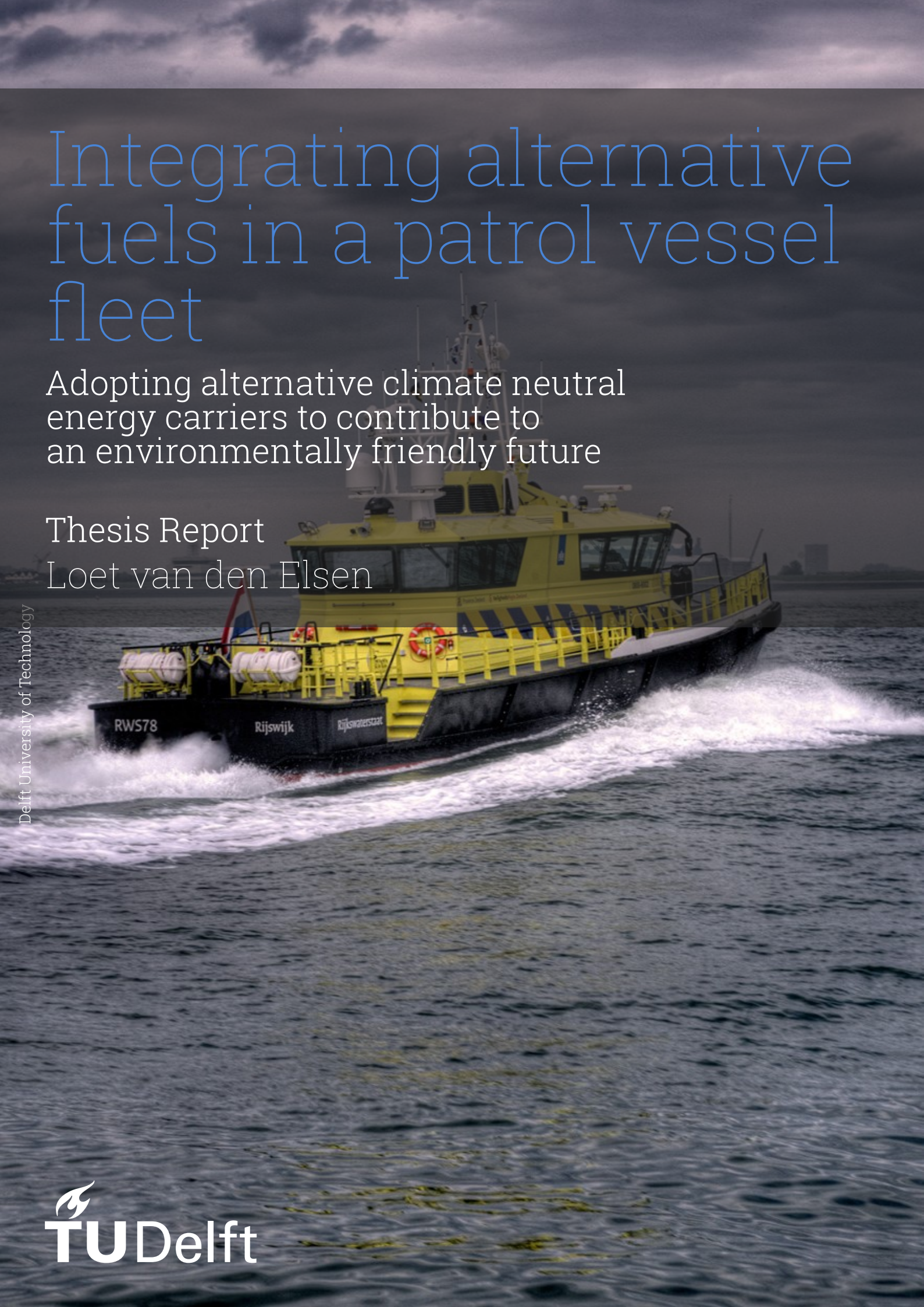

TU Delft

Thesis for the degree of MSc in Marine Technology in the specialization of Ship Design

Integrating alternative fuels in a patrol vessel fleet

Adopting alternative climate neutral energy carriers to contribute to an environmentally friendly future

by

Loet van den Elsen

Performed at Rijkswaterstaat

This thesis (MT.24/25.050.M) is classified in accordance with the general conditions for projects performed by the TUDelft.

Date of exam: 26-08-2025

Company supervisors

Responsible supervisor	Ir. L. Verheijen
	I

Thesis exam committee

Chair/Responsible professor:	Dr. Ir. P. de Vos
Staff member:	Ir. J.L. Gelling
Company member:	Ir. L. Verheijen

Author details

Studynumber:	4864891

Cover: *Mooi is ze hè?*. From “Facebook” by Rijkswaterstaat, 2024 (https://www.facebook.com/photo.php?fbid=879415220886798&id=100064549845673&set=a.138137415014586)

TU Delft

Rijkswaterstaat
Ministerie van Infrastructuur en Waterstaat

AI Statement

For this master thesis report I have not used Generative AI at all.

Summary

This thesis aims to determine which energy carrier is best suited for Rijkswaterstaat (RWS) patrol vessel fleet. RWS considers batteries, hydrogen and methanol (in that order of preference) as potential climate neutral energy carriers, as part of its goal to become a climate neutral organisation in 2030. Implementing these energy carriers, with low energy densities compared to diesel, into a patrol operation poses a challenge, because of the limited load carrying capacity and space on patrol vessels.

Through on-board observations, interviews with crew members and an operational supervisor, and AIS-data analysis, three distinct operating region types were identified. Region type I mainly covers rivers, with partially speed limited areas. Type II regions cover open waters and large rivers with no speed limitations. And regions of type III are areas that are almost exclusively speed limited. For each region type, the energy demand of an extreme 24-hour shift is estimated, with type III being the lowest and type II being the highest.

For each region type, five different configuration of power generators and energy carriers are analysed: fully battery-electric, a hybrid of batteries and hydrogen fed PEMFCs, a hydrogen fed ICE, a methanol fed ICE, and a battery-methanol ICE hybrid. The most important necessary elements in each power plant are identified, and the weight and size of each element is estimated as a function of the total installed power. This way, the total power plant weight and size can be calculated.

To enable testing of the feasibility of every configuration in each of the region types, the resistance of typical vessels operating in each region is estimated as a function of power plant weight. In regions of type I and II, planing hulls of current patrol vessels are used as a reference, and in regions of type III, a displacement vessel is used as a reference because of the speed limitations.

By iterating the power plant weight and the ship resistance, it was found that in type I and type II regions, a methanol ICE is the only feasible power plant configuration. In regions of type I, the main ship dimensions and the installed power have to be increased compared to the current vessels to enable climate neutral operation. For type II regions, additional measure are needed to enable operation on methanol. Decreasing the minimum time between bunkers, the maximum speed, or the vessel weight are to be considered. In type III regions, batteries are found to be a feasible option, with an increased vessel size and installed power compared to the currently operating reference vessel.

Next, a suggestion is made for the general layout of each vessel type. To account for the larger size of the machinery associated with the alternative energy carriers and power generating equipment, some accommodation space may need to be sacrificed to function as machinery space. In type I and type II vessels, storing methanol in the double bottom requires additional cofferdam weight, but vacates the space that is usually reserved for diesel tanks. In the type III vessels, it is suggested that the relatively heavy batteries are located amidships in between the machinery room and the accommodation space to prevent excessive trim. The space aft of the machinery room can be used for cooling systems.

The credibility of this thesis' results is subject to several factors. The operational profile and thus the total required energy demand of each region type is based on limited resources. Next, the weights of some power plant elements are hard to accurately estimate, and most are prone to changes because of future technological developments. Further, the availability and infrastructure of methanol and hydrogen might influence the feasibility as fuels for the patrol vessels. Next, the input values of the resistance calculations are estimations measured on the 3D models. More extensive tests are needed to provide more reliable approximations of the total resistance. Finally, ship stability may negatively impact the feasibility of the alternative energy carriers. In this thesis, no extensive stability check is performed.

Following this thesis, there are two main recommendations. First, RWS is recommended to look into potential changes in its operation and vessel designs to identify opportunities to decrease the energy demand of the vessels, like using cars if possible, constructing vessels using lighter materials, or using alternative hull types. Second, because of the global energy transition, it is recommended to follow technological developments and re-evaluate the feasibility batteries, hydrogen and methanol.

Contents

List of Figures

List of Tables

Nomenclature

Abbreviations

Abbreviation	Definition
DAC	Direct Air Capture
DoD	Depth of Discharge
DNV	Det Norske Veritas
FC	Fuel Cell
GHG	Greenhouse Gas
ICE	Internal Combustion Engine
IenW	Ministry of Infrastructure and Water Management
IPCC	Intergovernmental Panel on Climate Change
LCO	Lithium Cobalt Oxide
LFP	Lithium Iron Phosphate
Li-ion	Lithium-ion
LMO	Lithium Manganese Oxide
LNG	Liquefied Natural Gas
LTO	Lithium Titanate
MCFC	Molten Carbonate Fuel Cell
NCA	Lithium Nickel Cobalt Aluminium Oxide
NMC	Lithium Nickel Manganese Cobalt Oxide
PEMFC	Proton Exchange Membrane Fuel Cell
PM	Particle Matter
RWS	Rijkswaterstaat
SCR	SSelective Catalytic Reduction
SKAO	Stichting Klimaatvriendelijk Aanbesteden & Ondernemen
SOC	State Of Charge
SOH	State of Health
SOFC	Solid Oxide Fuel Cell
SSB	Solid State Battery
TNO	Netherlands Organisation for Applied Scientific Research
WBCSD	World Business Council for Sustainable Development
WRI	World Resource Institute
WTW	Well to Wheel/Wake

Chemical compounds

Abbreviation	Definition
CH_3OH	Methanol
CO	Carbon Monoxide

Abbreviation	Definition
CO_2	Carbon Dioxide
H_2	Hydrogen
N_2	Nitrogen
NO_x	Nitrogen Oxides
SO_x	Sulfur Oxides

Symbols

Symbol	Definition	Unit
a_{0-11}	Set of coefficients in DSDS prismatic polynomial	-
A_p	Projected planing bottom area	m^2
b_{0-11}	Set of coefficients in DSDS rocker and twist correction polynomial	-
B_{oa}	Beam over all	m
B_{px}	Maximum breadth over the chines	m
c_{margin}	Refuelling margin	-
$c_{time\ step}$	energy correction for asymmetry between shifts	-
$E_{req,8h}$	Required energy in an extreme 8-hour shift	kWh
$E_{req,24h}$	Required energy in an extreme 24-hour shift	kWh
$E_{stored,batt}$	Battery energy storage capacity	kWh
E_{stored,H_2}	Hydrogen energy storage capacity	kWh
E_{stored,CH_3OH}	Methanol energy storage capacity	kWh
F_∇	Displacement based Froude number	-
g	Gravitational constant	m/s^2
L_{oa}	Length over all	m
L_p	Length of projected planing bottom area	m
LCG	Longitudinal center of gravity from Ord. 10 as a percentage of L_p	-
m_{PP}	Cumulative weight of power plant elements	t
P_E	Effective towing power	kW
P_{FC}	Installed fuel cell power	kW
P_{ins}	Total installed power	kW
P_O	Open water propeller power	kW
P_P	Propeller power	kW
P_T	Thrust power	kW
r_{batt}	Share of energy stored in batteries	-
r_{CH_3OH}	Share of energy stored in methanol	-
r_{H_2}	Share of energy stored in hydrogen	-
R_t	Total ship resistance	N
T	Draught	m
t	Thrust deduction factor	-
$t_{refill,batt}$	Time between battery recharges	d
$t_{refill,CH3OH}$	Time between methanol bunkers	d
t_{refill,H_2}	Time between hydrogen bunkers	d

Symbol	Definition	Unit
V_{PP}	Cumulative volume of power plants elements	m^3
v_s	Ship speed	m/s
w	Wake fraction	-
β	Deadrise angle	°
Δ	Displacement weight	kg
ε	Deadrise angle at Ord. 10 minus the deadrise angle at Ord. 0	°
η_{batt}	Total battery efficiency	-
η_{DoD}	Depth of discharge margin	-
$\eta_{batt,electrical}$	Electrical efficiency of battery power plant	-
$\eta_{CH_3OH\,ICE}$	Total energy efficiency of methanol power plant	-
$\eta_{FC,electrical}$	Electrical efficiency of PEMFC power plant	-
$\eta_{FC,output}$	Chemical output efficiency of PEMFCs	-
η_H	Hull efficiency	-
$\eta_{H_2\,ICE}$	Total energy efficiency of an H_2 ICE power plant	-
η_O	Open water efficiency	-
η_{PEMFC}	Total PEMFC efficiency	-
η_R	Relative rotative efficiency	-
η_{SoH}	State of health margin	-
$\eta_{transmission}$	Transmission efficiency	-
γ	Average centerline angle form Ord. 10 to Ord. 0 w.r.t. baseline	°
∇	Displacement volume	m^3

1

Introduction

A climate neutral organisation in 2030. That means no net greenhouse gas emissions of any kind. The Dutch Ministry of Infrastructure and Water Management (IenW) imposed this goal on itself in 2018 (Rijksoverheid, 2022). The Rijksrederij, that manages the fleet of several governmental bodies like Rijkswaterstaat (RWS), has set the goal to make their fleet not only climate neutral, but also emission free if possible. To achieve this, it wants to adopt alternative energy carriers for its fleet consisting of more than 100 vessels, amongst which more than 30 patrol vessels. Batteries, hydrogen and methanol are considered as sustainable alternatives to fossil fuels (IenW, n.d.). These fuels are challenging to implement in a maritime operation that almost exclusively relies on fossil fuels. Research into the possibilities and limitations of each energy carrier is needed to establish which carriers hold potential in different use cases.

This thesis aims to provide insight in how the fossil fuel driven patrol fleet managed by the Rijksrederij can be transformed into a climate neutral and emission-free fleet by adopting less harmful alternative fuels as energy carriers. The following research question is to be answered:

How can the Rijksrederij patrol vessel fleet be turned climate neutral and preferably emission free within the operational demands, by adopting batteries, hydrogen or methanol as an energy carrier?

To answer the main research question, the following sub-questions will be answered:

1. *What are the patrol vessels' relevant operational requirements and what are the characteristics of the different patrol areas?*
2. *How does the adoption of the energy carriers influence the design requirements compared to a fossil fuel-powered vessel?*
3. *Which energy carriers are best suited for the Rijksrederij's patrol vessels?*

To get a better understanding of the RWS' operation, the day-to-day activities of several shifts are observed, crew members are interviewed, and AIS data of several patrol vessel is analysed. Using previous research into the refitting of existing patrol vessels, an evaluation is made of the necessary systems on board of a vessel powered by batteries, hydrogen or methanol. The specifications of some of these systems are provided in these research papers, others are based on products available on the online market.

Further, this thesis is a technical feasibility study in an early exploring stage of the new fleet, as it is expected that the first climate neutral patrol vessels will not be built before 2030. It is aimed to provide insight in which energy carriers are likely worth investigating further. Also, because of time constraints and price volatility, financial concerns are disregarded.

This report is structured as follows: chapter 2 provides a background into the definition of climate neutrality and current renewable energy technologies. In chapter 3 an overview is made of the regional differences in patrol vessel design requirements, operational profiles and crew preferences. In chapter 4 a estimation is made of the total power plant weight and size as a function of the installed power of a

vessel. Next, chapter 5 explains how the resistance of patrol vessels in different operational regions is estimated. In chapter 6, a feasibility study is used to identify the which energy carrier is most suited for which region type, and an example of a design layout is presented for each region. Finally, in chapter 7 the main research question in answered, and the thesis' limitations and subsequent recommendations are stated.

2

Climate neutral energy carriers

As a preparation for this thesis, a literature study was conducted to form a contextual background for this thesis. This chapter summarizes the relevant topics of the literature study. First, the definition of climate neutrality is explored in paragraph 2.1. Then, the current battery technology in the maritime sector is discussed in paragraph 2.2. Next, an analysis of the current hydrogen technology is given in paragraph 2.3. Methanol is the third energy carrier, discussed in paragraph 2.4. Then, in paragraph 2.5, the density and required energy of stored energy carriers is compared. Finally, in paragraph 2.6, some methods are briefly mentioned to decrease the total energy demand of patrol vessels.

2.1. Climate neutral & emission free

The Rijksrederij aims to turn its fleet climate neutral, and, if possible, emission free (IenW, n.d.). But while these concepts seem straightforward, there are some important intricacies to them. Many different factors come into play, such as production processes of the fuels, the amount of greenhouse gases (GHGs) emitted during operations and certain strategies to decrease the emissions. In section 2.1.1, the definition of climate neutrality according to the Intergovernmental Panel on Climate Change (IPCC) is discussed. In section 2.1.3, the concept of emission free is explained.

2.1.1. Definition of climate neutrality

The IPCC defines climate neutrality as follows: *'Concept of a state in which human activities result in no net effect on the climate system. Achieving such a state would require balancing of residual emissions with emission (carbon dioxide) removal as well as accounting for regional or local biogeophysical effects of human activities that, for example, affect surface albedo or local climate.'* (IPCC, 2018).

Carbon dioxide (CO_2) is mentioned as an example of emissions, but other GHG's also contribute to bio-geophysical effects of human activities on climate. The balancing of residual emissions is explained in a broader sense with the IPCC's definition of 'Net zero emissions': *'Net zero emissions are achieved when anthropogenic emissions of greenhouse gases to the atmosphere are balanced by anthropogenic removals over a specified period. Where multiple greenhouse gases are involved, the quantification of net zero emissions depends on the climate metric chosen to compare emissions of different gases (such as global warming potential, global temperature change potential, and others, as well as the chosen time horizon)'* (IPCC, 2018).

In order to balance the anthropogenic emissions of a company (or in this case a governmental body), one must determine how much the company emits in the first place. However, in many companies' climate neutrality targets indirect emissions are not taken into account, while this is often a significant share of the total environmental footprint (Kachi et al., 2020).

2.1.2. Direct and indirect emissions

The GHG Protocol was developed by the World Resource Institute (WRI) and the World Business Council for Sustainable Development (WBCSD) as a way for companies to effectively calculate their direct as well as their indirect emissions (WRI, WBCSD, 2011). IenW uses the CO_2 Performance

Ladder written by Stichting Klimaatvriendelijk Aanbesteden & Ondernemen (SKAO, 2020) to calculate their emissions in line with the GHG Protocol. This method can map and effectively reduce its emissions. The ladder makes a distinction between three scopes of emissions. Applied to the organisation of IenW, these scope are defined as follows.

Scope 1 emissions are direct emissions produced by property of IenW, for example as a result of burning diesel or gas for heating buildings or driving vehicles like the Rijkswaterstaat vessels. Scope 2 emissions are indirect emissions that are induced by IenW demand, but not produced by IenW owned installations. This mainly consists of electricity usage in buildings and by electric vehicles. Scope 3 emissions comprise business transportation, whether that be by private car, public transport or by plane (IenW, 2023a).

The CO_2 Performance Ladder specifically mentions that Well To Wheel/Wake (WTW) numbers must be used when calculating emissions, so emissions of producing, transporting and storing fuels must be taken into account (SKAO, 2020). This for example means that the climate neutrality of methanol depends on whether it was produced using renewable biomass and electricity. Analogously, while electric vehicles do not directly emit GHG's, they are not climate neutral if the electricity they run on is generated by burning fossil fuels. In accordance with the 'trias energetica' strategy, IenW aims to save energy, use electrical energy and generate its own sustainable energy where it can. Initially, IenW even set the goal to become energy neutral, meaning it wanted to generate all energy that the organisation used by itself. This goal, however, proved to be too ambitious and has since been dropped (IenW, 2023b). This means that the footprint of the organisation is dependent on the grade of sustainability of other parties that produce electricity and energy carriers for IenW. Whether or not the current electricity originates from renewable sources is outside of the scope of this thesis. In case the electricity used today is not renewable yet, the electrification of vehicles is a necessary step in preparation of a future in which the share of renewable energy is growing. Or in other words: the potential of an (emission-free) battery-powered vessel to be climate neutral is larger than that of a diesel-powered vessel.

The Ladder adheres to a comprehensive list of CO_2 emission factors of a wide variety of energy carriers in kg of CO_2-equivalent per unit of energy carrier produced, posted on co2emissiefactoren.nl (2024). According to this list, electricity generated through wind, water and sun energy has no emissions whatsoever (disregarding the construction emissions of wind turbines, water dams and solar panel fields) and grey and green hydrogen currently produce about 12.5 kg and 1.1 kg of CO_2-equivalent per kg of hydrogen respectively. These values are subject to the chosen transportation and storage methods of the hydrogen, as well as the type of electricity used in production. If renewable electricity is used, these values could theoretically drop to zero.

For methanol it is hard to determine the current CO_2 emissions factor, since it can be made through many different pathways as described by the Methanol Institute (Methanol Institute, 2022). Two sustainable examples are e-methanol, which is made with green hydrogen, and bio-methanol, which is made using biomass (wood, manure, crops or municipal waste among other things). These production pathways have a wide range of associated carbon footprints, with some even being negative meaning more GHGs are removed than produced.

2.1.3. Definition of emission free

To become climate neutral, one has to consider the CO_2 equivalent emissions of an energy carrier to be able to adequately compensate them, as discussed in section 2.1.1. But the Rijksrederij has the additional aim of employing emission-free vessels. An emission free vessel in this case is a vessel that does not emit any GHGs or particle matter (PM) in situ during operation. So while, for example, batteries, hydrogen and methanol have the potential of being climate neutral, batteries and hydrogen are still preferred over methanol since they are free of emissions in operation (neglecting the H_2O emissions from hydrogen fuel cells).

2.2. Battery technology

The preferred energy carrier of the RWS are batteries, because they are emission free in operation, and climate neutral if the electric energy in them is generated using renewable sources like wind turbines or solar panels. In section 2.2.1 relevant characteristics of current li-ion battery types are discussed. In section 2.2.2 solid-state batteries are discussed.

2.2.1. Lithium-ion batteries

Today, lithium-ion batteries are used in many applications and are a key component in vehicle electrification. Six types of li-ion batteries are mainly used, each distinguished by the materials the cathode and anode are made out of. Different material configurations possess different characteristics, like energy density, charging speed, safety and availability, and thus suit different applications (flashbattery.tech, n.d.; Melançon, 2023; Miao et al., 2019). These six types are:

- **Lithium Cobalt Oxide (LCO)**: the LCO battery is commonly used in electric mobile devices because of its high energy density, long life cycle and ease of manufacturing. They are, however, prone to overheat under high loads, making them unsuitable for larger applications that demand high loads like electric vehicles from a safety stand point. Also, cobalt is toxic and cobalt supply is limited, making it attractive for manufacturers to look for alternative li-ion battery materials (flashbattery.tech, n.d.; Miao et al., 2019).
- **Lithium cobalt oxide (LMO)**: LMO batteries have a low internal resistance, allowing for fast charging and discharging, the latter meaning it can deliver high power and they have better thermal stability than LCO batteries. However, they have a 33% lower capacity than LCO and significantly lack behind in terms of life span (Miao et al., 2019).
- **Lithium Iron Phosphate (LFP)**: LFP batteries have a low resistance and high current rating, as well as a long life span. They have a good thermal stability, so they are not likely to overheat and catch fire. A caveat is the relatively high self-discharging rate over time, which can be mitigated with additional control electronics, adding to the battery pack size and weight. Also, LFP batteries have a shorter life span when exposed to moisture (Miao et al., 2019). But while it is harder to recycle these batteries, an advantage is the lack of need for rare metals, like cobalt and manganese, VPRO Tegenlicht reports (2024).
- **Lithium nickel manganese cobalt oxide (NMC)**: The combination of nickel and manganese in these batteries makes for batteries with high specific energy and thermal stability. Because of this, these batteries are in high demand (Miao et al., 2019). In recent years, manufacturers have been decreasing the cobalt and manganese content of these batteries to decrease cost and increase energy density, but this proves challenging since cobalt provides stability and increases life span (flashbattery.tech, n.d.).
- **Lithium Nickel Cobalt Aluminium Oxide (NCA)**: Just like NMC batteries, NCA batteries provide high specific energy and power and a long life span. However, they lack safety and need extra safety measures to use them in ships. Also, they are more expensive than NMC. An advantage with respect to NMC is that they can contain even less cobalt (flashbattery.tech, n.d.; Melançon, 2023; Miao et al., 2019).
- **Lithium Titanite (LTO)**: The last li-ion battery type is the LTO battery, which excels in terms of total charging cycles, safety properties and charging speed. However, they have a low energy density and are currently expensive (flashbattery.tech, n.d.; Melançon, 2023; Miao et al., 2019).

Applications of lithium-ion batteries

NMC and NCA batteries are commonly used in the automotive sector because of their high energy and power density. The total number of life cycles is of less importance, since cars usually do not exceed a total of around 2000 charging cycles through their life span, which is within the life span of these batteries (flashbattery.tech, n.d.; Miao et al., 2019). When used in a marine vessels with a higher count of charge cycles during its service life, the battery packs will probably need to be replaced at some point or several points throughout the years.

LFP and LTO are used in industry, agriculture and special vehicles where service life, reliability and safety are important requirements and energy density is not a priority (flashbattery.tech, n.d.; Miao et al., 2019).

LCO and LMO are usually used in small applications where energy density is not much of an issue since it can only influence the application on a small scale. Also, safety is less of an issue here because the total application is small and thus the risk (probability times consequence) of thermal runaway is small (flashbattery.tech, n.d.), but it has been used in some EVs (Miao et al., 2019).

While li-ion batteries can play a crucial role in the green energy transition, Guillaume Pitron mentions in an episode of VPRO Tegenlicht (2024) that it is important to realise that the mining of rare metals,

like cobalt and manganese, also comes at an environmental price. And that this price is currently being outsourced to the countries that produce the metals, while the consumers, like EV owners, are not aware of the environmental cost in countries like Congo or China. Pitron is not opposed to the electrification of the world; 'I want to have the energy transition taking place as soon as possible', he states. But in choosing a battery type, rarity of metals is something to take into consideration. Subsequently, recycling plays an important role in easing the pressure put on the environment. Pitron mentions the LFP battery as a positive development, since its production requires less rare metals than the other battery types.

2.2.2. Solid-state batteries

While li-ion batteries have been well established as an energy carrier in the electric application market, a lot of research is currently being put into solid-state batteries (SSBs). Current developments are promising and they are a real contender to replace li-ion batteries in the future.

The main difference of SSBs compared to li-ion batteries is the use of a solid material as an electrolyte. This presents a lot of advantages with respect to li-ion batteries: a great improvement in material stability increasing the service life time and decreasing formation of dendrites, that can cause short circuiting in the long term. Also, a solid electrolyte is far less flammable than a liquid electrolyte (Kartini & Genardy, 2020; Yu et al., 2023). Furthermore, SSBs have higher energy densities compared to li-ion batteries.

Still, SSBs have some challenges to overcome. With a solid electrolyte, it is hard to maintain a stable conductive interface between the electrodes and the electrolyte, which causes conductive inefficiencies, or i.e. a lower (dis)charge rate and power density (Kartini & Genardy, 2020).

Extensive research into many different types of electrode and electrolyte materials is needed to establish SSBs as a long-term energy carrier. Added to this is the need of a production breakthrough, since SSB production processes are not suited for large scale production yet. Industrial concerns, like prices, waste, boiling points, viscosity and toxicity, are still unclear and are dependent on the production process. But many production methods are still being explored (Janek & Zeier, 2023). Subsequently, the market for SSBs is young and in full development.

In the next five to ten years, a variety of SSB pilot production projects are expected, which have to show SSB competitiveness or superiority on a large scale. For now, not all companies are willing to announce their future production capacity of SSBs. It is expected that different kinds of SSBs will enter the market at different times in the coming years. In 2030, expected available energy densities range from 340 Wh/kg and 770 Wh/L up to 440 Wh/kg and 900 Wh/L, with even further improvement after that (Wu & Wu, 2023). Another study predicts a range of energy densities from 275 Wh/kg and 650 Wh/L up to 445 Wh/kg and 905 Wh/L around 2030 (Schmaltz et al., 2023).

2.3. Marine hydrogen technology

Hydrogen is RWS' second preference for climate neutral and emission-free energy carriers. Using hydrogen as an energy carrier has its own advantages and challenges compared to batteries and fossil fuels. Some of the main considerations when operating a vessel using hydrogen are discussed in the following. Paragraph 2.3.1 discusses the chemical forming of hydrogen and the future availability of hydrogen. In section 2.3.2 storage of compressed and cryogenic hydrogen are discussed. Next, in section 2.3.3 the two main methods of energy conversion of stored hydrogen are explained. Lastly, in section 2.3.4 the most important safety considerations regarding hydrogen storage are mentioned.

2.3.1. Hydrogen production and availability

Currently, there are two established large scale production methods for hydrogen, namely reforming of methane and water electrolysis (Van Hoecke et al., 2021). These reactions are net endothermic, thus external energy is put into the system (Van Hoecke et al., 2021). (Since a fuel is a chemical energy storage, the production process of a fuel is endothermic.) Producing the external input energy with renewable energy, as is the case with green hydrogen, is an important step in becoming climate neutral.

To implement hydrogen in the maritime sector, some serious upscaling is still called for, as stated by the Netherlands Organisation for Applied Scientific Research (TNO, n.d.). TNO explains that in 2020 200 MW of hydrogen electrolysis plants were installed globally, while in 2023, this number had grown

to 2400 MW. These numbers show the need for the development of an entirely new supply chain. The goal of the European Union is to have 40 GW installed in Europe, and another 40 in North Africa in 2030.

According to the Dutch climate agreement of 2019, the industry and harbours need to have a capacity of 3 to 4 GW in 2030, and a capacity of 8 GW in 2032. This capacity does depend on the development of energy generation capacity of wind turbines at sea, electric grid infrastructure and energy demand of end users (Elzenga & Strengers, 2024).

2.3.2. Pure hydrogen storage

Storage of hydrogen is one of the main challenges that hydrogen faces to replace fossil fuels. Hydrogen gas at atmospheric pressure and room temperature has an energy density of roughly 0.01 MJ/L, which is less then 0.03% of the energy density of diesel (Demaco, n.d.). In this section the two common ways of storing hydrogen with higher density are discussed: pressurised and liquefied.

Compression is one of the two common ways to store hydrogen. This can be done in type I through type IV vessels, with type V not being available on a large scale. The vessel types with higher Roman numerals have higher complexity, from a pure steel tank to a polymeric liner fiber-wound tank. The pressures in these tanks go up to 700 bar. Types I and II are typically not suitable for vehicle applications, because of their heavy weight and hydrogen embrittlement over time, while types III and IV are more expensive but have less issues regarding weight and cracking (AlZohbi et al., 2023; Li et al., 2024). The pressurised hydrogen has a density of about 40 kg/m^3 (Demaco, n.d.) and pressurising costs about 10% of the of the energy content of the stored hydrogen (Van Hoecke et al., 2021).

The second method to store hydrogen with an increased energy density is through liquefaction. The hydrogen is cooled down to below its boiling point of -253°C, where it has a density of roughly 71 kg/m^3. Then, it is stored in large spherical or cylindrical tanks. Storing hydrogen in its liquid form does come with some prevalent disadvantages.

First, it takes up a lot of space. Even though the density is 75% higher than that of pressurised hydrogen, the energy density is still only a quarter of diesel's energy density (Van Hoecke et al., 2021). Second, liquefying hydrogen requires a lot of energy: about 30% of the total energy of the stored hydrogen (AlZohbi et al., 2023; Li et al., 2024; Van Hoecke et al., 2021). Third, liquids that are highly flammable or very cold have inherent safety concerns. This means additional measures must be taken to mitigate safety risks. Fourth, over time heat is absorbed through the tanks, causing part of the hydrogen to evaporate; this is known as boil-off. However, boil-off is less of an issue for patrol vessels, since they can be designed to sail on the boil-off gas (Van Hoecke et al., 2021).

2.3.3. Energy converters

Hydrogen can be used in fuel cells (FCs) as well as in an internal combustion engine (ICE) to deliver power. Both power converters have advantages and disadvantages which will shortly be discussed here.

Fuel cells

Fuel cells generate electricity using hydrogen. This means that a ship powered by fuel cells has to be electrified, whereas an engine delivers mechanical energy to the propeller. Currently, the proton exchange membrane fuel cell (PEMFC) is widely used in hydrogen systems, but these fuel cells require extensive purification of the hydrogen supply stream, because very low levels of ammonia (NH_3) and carbon monoxide (CO) are enough to poison the cells. Molten carbonate fuel cells (MCFC) and solid oxide fuel cells (SOFC) operate at such high temperatures, that NH_3 and CO decompose. Because of this, fuels like ammonia and methanol can be used directly in the fuel cells. However, at these temperatures formation of nitrogen oxides (NO_x) is an issue. Compared to ICE, FCs are more expensive and typically have a shorter lifetime. An advantage of fuel cells is that they can operate emissionless (disregarding H_2O) at low temperatures (Van Hoecke et al., 2021). Added to this, FCs typically have an efficiency of 50-60%, whereas ICEs operate at about 40% and FCs have minimal vibration and noise levels (Li et al., 2024).

Internal combustion engine

To use hydrogen in an ICE, either spark ignition is needed or it must be used in a dual-fuel (currently usually with diesel) configuration, because of the high auto-ignition temperature of hydrogen. An advantage of using ICE is the familiarity of its implementation in ship designs. However, hydrogen-powered ICEs have a low power output and a gradual transient response, making them less suitable as the main driver of a vessel (Li et al., 2024). Furthermore, because of the high auto-ignition temperature NO_x is produced, making this method of using hydrogen less sustainable. Also, the hydrogen powered ICEs in general still need a lot of research to increase efficiency to a level at which they can compete with diesel engines (Dere, 2023).

2.3.4. Safety considerations for hydrogen usage

Since hydrogen has an inherent explosion risk, and hydrogen permeation over time is an issue, safety is an important factor in the vessel design. Det Norske Veritas (DNV) reports important measures to decrease hydrogen storage related risks, some of which are shortly mentioned in the following: first, when high-pressure storage tanks are placed in the open above deck, leaking hydrogen will disperse decreasing cloud size and explosion severity is decreased in open spaces compared to confined spaces. However, the storage tanks are more exposed when stored on deck and leakage is harder to detect. Because of this, storage under deck might be preferred, but this requires other safety precautions: manned spaces and critical areas must be shielded from possible explosions or leakage by creating distance, placing strong walls and adequate ventilation around storage rooms. Leakage is an issue mostly concerning compressed hydrogen because of the number of valves, the size of the tanks and, evidently, because of the higher pressure. Liquid hydrogen leaks are, however, more severe because of the danger to humans and damage to structures that low temperature liquids can afflict. It is desirable to have several storage units separated by valves to decrease the potential leakage, and thus explosion or fire size (DNV, 2021).

2.4. Marine methanol technology

Methanol (CH_3OH) has a well established global production network, with a global production of roughly 111 million tons in 2022 (Methanol Institute, n.d.-b), of which about 3.5 million was produced within the EU-27 and in Norway (Wissner et al., 2023). Methanol contains carbon atoms that will be emitted as CO_2 among other things at the end of the fuel's life cycle. The environmental impact of methanol is therefore not only dependent on renewable production energy, but also on the source of CO_2 in the production process. In the short term, CO_2 from biomass, like municipal waste, and extraction from industrial point sources can be used. In the long term, direct air capture (DAC) can be used, but this technology is not yet as advanced as nitrogen separation from the air used for e-ammonia production (Wissner et al., 2023).

However, compared to other renewable fuels, methanol has a high gravimetric and volumetric energy density (Van Hoecke et al., 2021). Also, liquid methanol can be stored and bunkered at room temperature and ambient pressure, eliminating the need for special tanks (Zincir & Deniz, 2021). Furthermore, internal combustion engine technology for methanol is more mature than that for hydrogen and has an engine efficiency similar to that of diesel engines. Methanol does only work in designated ICEs with either spark-ignition or a pilot fuel. A very prominent advantage of methanol engines compared to diesel engines is the decrease in emissions; CO_2 emissions decrease moderately, while NO_x, SO_x and particle matter (PM) emissions decrease severely (Zincir & Deniz, 2021). The emission decrease of the last two is reported to be as high as 98% and 90% respectively (Wissner et al., 2023).

An important consideration is that methanol is toxic to humans, and it can be absorbed by inhalation, ingestion and skin contact. An upside is that 'acute danger for maritime life due to methanol spills is highly unlikely', since 'methanol is hardly toxic for fish, invertebrates, algae and microorganisms in the short term'. Moreover, 'methanol is fully biodegradable with no potential to bioaccumulate' (GESAMP, 2019 as cited in Wissner et al., 2023).

Lastly, if methanol is cracked to release H_2, it can be used in fuel cells, allowing for flexible power generation from a single chemical energy storage compound. This does require a methanol cracking installation on board. For now, fuel cells are likely to enter the market in hybrid systems, and powering ships solely with fuel cells is projected to become an application in the long term (Wissner et al., 2023).

2.5. Storage efficiency and density

To select the most suitable storage method, the energy densities of each carrier must be considered, as well as the energy required to produce those carriers. Furthermore, each carrier has its own associated storage requirements, like pressurised tanks, cryogenic tanks, safety equipment, and temperature regulators.

Figure 2.1 shows a schematic of the energy consumption of several storage methods of hydrogen, both in its pure form and in different chemical compounds. The initial production of hydrogen by electrolysis is the most energy intensive step in every storage method process, depicted by the red parts. Therefore, to minimise the total required energy, it is important that as little hydrogen is lost through the rest of the process as possible. This explains why synthetically manufactured FT-diesel (Fischer-Tropsch diesel) is so inefficient: in the first step of its production process, H_2 and CO_2 react to form H_2O and CO. In the second step, this CO reacts with H_2 to form even more H_2O and a hydrocarbon chain in the form of C_nH_{2n+1}. So for every H_2 effectively stored in a hydrocarbon fuel, two H_2 molecules are lost in the production of unused water.

The figure shows that liquid and compressed hydrogen belong to the most efficient hydrogen storage systems; energy is only needed for the production of the hydrogen and converting it to the requisite storage conditions. Five carriers have a part of the energy dedicated to 'H_2 release'. This means energy is needed in order to extract the H_2 from the carrier, and it is assumed that the needed energy is taken from the chemical energy stored in the fuel itself, and that no waste heat recovery system is employed (Van Hoecke et al., 2021).

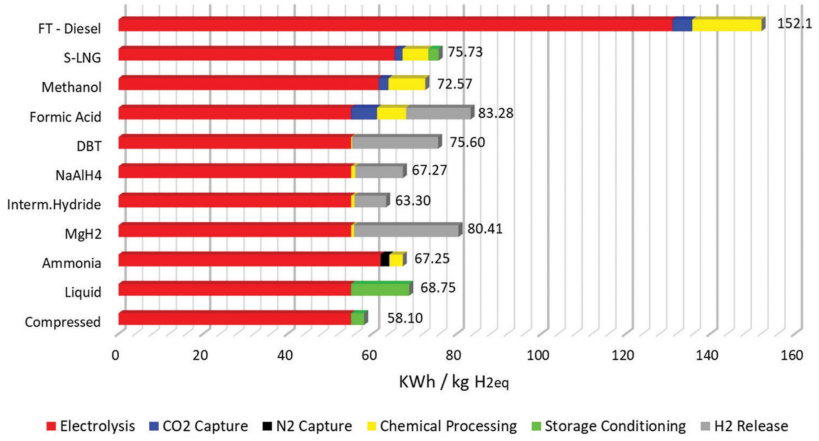

Figure 2.1: Energy required for the production and storage with associated losses in kWh/kg of stored H_2 (Van Hoecke et al., 2021).

In figure 2.2 the energy densities of the carriers are shown, both with and without their designated storage tank. Pure hydrogen has a very high gravimetric density on its own, but the tanks needed to maintain storage conditions are large and heavy. Methanol and ammonia are fairly similar in terms of density, both with and without tanks. As can be seen, diesel and LNG still outperform every other carrier by a large margin in terms of in-tank weight and volume, apart from methanol (Van Hoecke et al., 2021).

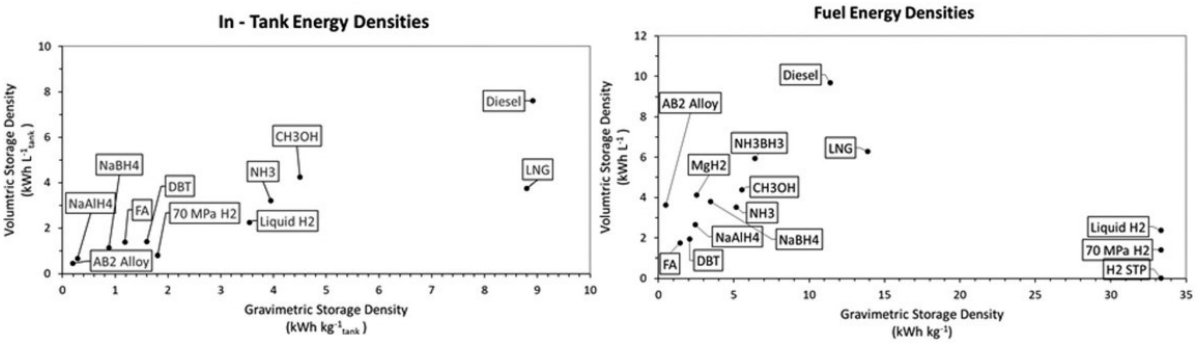

Figure 2.2: Energy density of pure H_2 storage substances and their energy density when stored in dedicated tanks (Van Hoecke et al., 2021).

2.6. Energy saving measures

An important step in the process of becoming climate neutral is to adopt energy saving measures. This comes with several advantages. For one, it is trivial that consuming less energy in itself is a step towards climate neutrality. But next to this, if vessels require less energy in operation, they do not have to carry as much fuel. And since energy density is one of the great challenges of renewable energy carriers, having to carry less may enable implementation of them on vessels on which it would otherwise not be possible. Third, saving fuel means saving money, which in an advantage in itself. But analogous to density, lower prices can lead to faster adoption of renewable fuels and technologies.

The International Renewable Energy Agency has explored a '1.5°C scenario', in which renewable fuels make up a 70% share of all global shipping fuels, with an 80% decrease in global shipping emissions. Of this emission reduction, 60% is due to adoption of alternative fuels, and 20% is due to more energy efficiency on board (IRENA, 2021). It must be noted that it is hard to estimate to what extent the global shipping industry is representative of a patrol vessel fleet, but this does provide some insight in the importance of energy efficiency and on-board energy savings.

In this chapter, several energy saving measures are discussed that can be implemented in patrol vessel designs. First, section 2.6.1 explains how hybrid energy systems can enable the operation of a vessel in multiple design conditions. In section 2.6.2 the importance of hull form selection is explained. Section 2.6.3 discusses how hydrofoils can be used to decrease resistance and wave generation at higher speeds. Section 2.6.4 discusses the potential relevance of a multihull design. Lastly, section 2.6.5 shortly discusses how a hull vane can be used to decrease wave generation.

2.6.1. Hybrid energy systems

As all discussed energy carriers have different energy densities and can be used in fuel cells, combustion engines or in some cases both, they all suit different ship types and operating conditions. Patrol vessels typically have quite distinctive operating modes: most of the time they are sailing at a relatively low speed. However, they must also be able to travel great distances at high speeds. It can be a great challenge to find a single energy carrier that meets the requirements for both operation modes.

Hybrid power systems can supply the advantageous features of reliable high-power and low-power operation. It can combine the good characteristics of several green energy sources to enable green operation across several operating modes. This can effectively reduce the energy consumption and emissions of a vessel (Yuan et al., 2020).

2.6.2. Hull shape

The hull shape of the vessel is crucial for the resistance of the ship. Wave making resistance is high when most of the ship is carried by the static buoyancy force. With the right hull shape, high speeds can lead to hydrodynamic forces that lift the vessel out of the water, decreasing the wave making resistance and the wetted surface area, on which the friction resistance is dependent. A V-shaped hull with a hard chine softens vertical and pitch accelerations and decreases slamming. Further, it ensures lower speed loss in waves, and increases course stability (Yun & Bliault, 2012).

2.6.3. Hydrofoil

Another way to reduce the fuel consumption, or, in essence, to increase the range of a vessel with a certain amount of fuel storage capacity, is by lifting it out of the water with hydrofoils. Up to 40 kn, high-speed craft with foils will have low fuel consumption compared to planing monohulls. Furthermore, planing vessels will make less waves, making them more useful in areas with protected nature and waterborne objects like houseboats. A challenge of hydrofoiling monohulls, however, is that they have to overcome a resistance peak at low speed just before lifting out of the water (Yun & Bliault, 2012). This challenge can be overcome by using batteries and fuel cells in a hybrid power system: fuel cells can deliver a steady power supply, and when there is a transient load, batteries can provide the additional power to lift the vessel out of the water, and use part of the fuel cell power to charge when power demand is low again (Jung et al., 2024). In figure 2.3,

Figure 2.3: The foiling Artemis EF-12 patrol vessel operating on the Nieuwe Maas river in Rotterdam (Artemis Technologies, n.d.)

2.6.4. Multihull

A lot of high speed craft, like passenger ferries, use multiple hulls. This is because multihulls have decreased wave making resistance due to their high length/beam ratio. A catamaran typically has the most resistance advantage at a Froude number of around 0.6-0.95. Moreover, catamarans have far better transverse stability and have increased deck area.

A disadvantage of a multihull is the limited load carrying capacity, because the hull is relatively heavy in comparison to a monohull, and the waterplane area is smaller. Also, catamarans are relatively wide (Yun & Bliault, 2012), which can be a limitation for patrol vessels that have to be able to enter small harbours.

Figure 2.4: The Incat Crowther 19, a 19 m long catamaran patrol vessel (Incat Crowther 19, n.d.)

2.6.5. Hull vane

A hull vane is a wing attached underwater to the stern of a vessel. It can significantly reduce fuel consumption by creating lift, correcting trim, reducing transom wave height and dampening pitch motions when sailing in waves. However, the vane can decrease manoeuvrability, and the hull vane increases the hull's draught, which can be a problem regarding a patrol boat's vessel size restrictions to enter harbours. This must be taken into consideration (Stark et al., 2022). Further, a hull vane can increase a vessel's resistance at speeds other than the vane's design speed, which might lead to an increased overall energy consumption.

3

The RWS Operational Framework

In order to know how adoption of an alternative energy carrier impacts the operations of the Rijkswaterstaat, the current operational patrol profile of the fleet must be mapped out. This chapter presents an overview of the current operations of the patrol vessels. This overview is based on on-board observations of four 8-hour shifts, conversations with crew members and an operational supervisor of the RWS, data from the Marad fleet management software and an AIS-data analysis of 6 RWS patrol vessels across the entire year of 2023.

In paragraph 3.1 3 region types are defined in order to generalise the design problem. Then, in paragraph 3.2 the energy demand in for each region type is estimated.

3.1. A diverse fleet covering 3 region types

Currently, the Rijksrederij fleet consists of 100 vessels, amongst which a little more than 30 patrol vessels. More than half of these vessels are unique within the fleet, which means there is a wide variety of ship types. The ranges of different main ship parameters is shown in table 3.1.

Table 3.1: The range of main parameters of the current patrol vessel fleet

Parameter	Range within fleet
Length over all	13.55m - 23.95m
Beam	3.85m - 5.67m
Draft	1.10m - 1.60m
Maximum speed	13.50kn - 33.00kn
Vessel age	11y - 43y

A downside of this high level of diversity is that crews have to get accustomed to and switch between many different ships. Furthermore, with increasing vessel age, dock repairs become more frequent, which leads to a lower employment rate across the fleet. RWS therefore intends to replace old vessel as soon as possible.

However, some level of diversity is needed among the fleet to meet the different regional requirements. From conversations with different crews in different operating regions, it is concluded that ship preferences differ from one region to another, depending on tasks to be performed and wave sensitivity of the area. Crews described the local wave sensitivity to be the main speed limiting factor. Even in cases of emergency, they will limit their speed as not to cause dangerous situations or damages in their trail. Depending on the day of the week, and the risk of calamities in the area, each region has its own deployment rate.

For this research, three distinct types of operating region are defined. These patrol regions are described in table 3.2 with their respective characteristics.

Table 3.2: Definition of the three general operating region types

Region	Quay wave sensitivity	Speed limit	General waterway type	Example regions	Hours deployed
Type I	Low - Medium	$\leq 22kn$	Large rivers	Maas, Waal	16 - 24 h/day
Type II	Low	$22kn$	Large open bodies of water	Markermeer, Westerschelde	16 - 24 h/day
Type III	Medium - High	$\leq 11kn$	Canals, Protected nature, Small lakes	Eemskanaal, Biesbosch, Bordering Lakes	8 - 16 h/day

In regions of type I, crews mostly prefer a vessel like the RWS 21, depicted in figure 3.1a. This vessel is 18.8 m long, and has a beam of 5.25 m and a draught of 1.25 m. This size allows crews to manoeuvre easily in smaller spaces like harbours, but is still large enough to board inland cargo vessels and provides enough space inside to operate with 3 or 4 people. The RWS 21 has an installed power of 970 kW, allowing them to overcome the hump speed and reach up to 22 kn without wind and waves. Some crew members mentioned the larger RWS 70-series as a good alternative to the RWS 21 in type I regions.

In regions of type II, higher waves can be expected and a larger vessel is required to prevent large roll and pitch angles and accelerations. According to the crew and based on observations during a shift on the Markermeer, the RWS 70-series ships are the minimal size for operation on these waters. The RWS 77 is shown in figure 3.1b. These vessels are 23.95 m long, 5.59 m wide and have a draught of 1.32 m. With an installed power of 1302 kW, these vessels can reach a maximum speed of 24 kn.

Vessels in regions of type III are not required to sail fast. These vessels therefore do not need as much power and as much of a sharp V-shaped hull as the other 2 types. The canals in Groningen (a type III region) are currently patrolled by the RWS 59, which is depicted in figure 3.1c. It has a length of 19.45 m, width of 5.3 m and a draught of 1.4 m, and it can reach a maximum speed of 20 kn. The AIS-data analysis shows that this vessel has never exceeded a speed of 12 kn in the year 2023, and it mainly operates at a speed of 7 kn. The new generation of ships operating in type III regions might require a lower installed power than the RWS 59.

For all regions, the maximum draught of a vessel may not exceed 1.4 m.

(a) RWS 21 operating on the Dordtse Kil (Hemken, 2025)

(b) RWS 77 operating on Urk (Heidinga, 2021)

(c) RWS 59 operating near Wijhe (Heidinga, 2020)

Figure 3.1: Three example vessels that fit a specific region type

3.2. Energy demand in different operational modes

In the previous paragraph, three general operating region types have been defined. In this paragraph, the power and effective energy demand of ships patrolling the three region types are estimated. To this extent, 6 different operating modes are defined:

- *Crew switch:*
  On the patrol vessels, days are divided into 3 shifts of 8 hours. Crews usually start their shift by discussing the tasks to be performed, checking off a list of inspections in the engine room and, if necessary, administrating. This takes between 30 minutes to an hour. When all patrol tasks have

been finished and the end of the shift closes in, crews will get back to the harbour, usually with some time margin before the next crew starts. This margin is usually around 45 minutes to an hour.

- *Moored/Refueling/Inspection:*
  During a shift, crews may moor their vessel at a bunker station to refuel, at one of the vessel traffic posts to pick up supplies or in a harbour to carry out inspections or to have dinner.
- *Calamity/Lock:*
  When crews operate near an emergency site, they will limit their speed to ensure safe operation and to prevent additional hazards. Examples of emergencies could be to haul potentially dangerous floating objects to shore or to aid damaged ships.
- *Low speed:*
  Most of a patrol is spent cruising at a relatively low speed. In this mode, the vessel is usually travelling to a certain target destination or patrolling the waterways for the sake of being present and visible and to look for irregularities. In this operating mode, crews adjust their speed to save fuel and to prevent wave nuisance. In-transit inspections on board of travelling inland vessels are also done at this speed. In region types I and II, speeds close to 9 knots are considered low, and for type III regions, speeds of around 6 knots are considered low.
- *Intermediate speed:*
  Crews may choose to sail faster than their regular speed for several reasons. For example, if they need to get to a calamity, but are currently in a wave sensitive area, they are restrained from sailing at their maximum speed. Or when a large distance must be covered in a limited amount of time like in a single shift, medium speeds are necessary. A speed of around 16 knots is considered intermediate in type I and II regions, while intermediate speed in type III regions is around 10 knots.
- *Maximum speed:*
  Maximum speed is only sailed for longer periods on end in cases of emergency in areas not sensitive to waves. In regular shifts, crews on occasion sail at maximum speed to fully load the engine in an attempt to clean any carbon build up in the filters. The AIS data analysis shows, that in about 80% of all cases in which full speed is reached, it is maintained for a maximum of 5 minutes on end. In regions of types I and II, maximum speed is around 24 knots, while in type III regions, the maximum considered speed is roughly 12 knots.

In every operating region, there is a characteristic distribution of time spent in each of the operating modes. Based on on-board observations and crew statements, two extreme operational scenarios are determined in each region type: one for a dense shift schedule and one for a shift schedule with more off-time. Also, first estimates are made of the shaft power and the auxiliary power corresponding to each operating mode. Throughout this report, multiple calculations are done synchronously. For clarity, tables are assigned a separate colour that corresponds to its operational region.

To obtain better insight in the operational conditions of its fleet, RWS has hired external parties to measure the shaft power, torsion and on-board vibrations and sound levels as a function of the vessel's speed. In paragraph 3.1, the RWS 21 was mentioned as a suitable vessel for operations in type I regions. On the RWS 82, a vessel similar to the RWS 21, JVS Noise and Vibration Engineers has measured the shaft power across its entire speed range. Next to the shaft power, the auxiliary power must be determined. An Onan MDKDV (19 kVa) is currently installed in the RWS 21, with a maximum power output of 19 kW. For an extreme operational scenario, it is assumed that this generator is running at full power, except when crews are switching. In table 3.3, the total power demand in a type I region across an extreme 24-hour scenario, or $E_{req,24h}$, is shown.

Table 3.3: An extreme operational scenario in a type I region. The power estimations are based on the

Extreme 24 hours:						
	Local operation			Transit		
Operation mode	*- Crew switch - Off-duty*	*- Moored - Refueling - Inspection*	*- Calamity - Lock*	*- Cruising speed - Mobile Inspection (∼20 km/h)*	*Intermediate speed (∼30 km/h)*	*Max speed (∼45 km/h)*
hours	6	1	2	6	5	4
power (kW)	0	19	38	199	485	909
energy (kWh)	0	19	76	1194	2425	3636
				Total per day:	**7350**	**kWh**

In type II regions, crews prefer vessels like the RWS 70-series. In 2023, Maritime Research Institute Netherlands (MARIN) measured the shaft power on board of the Damen StanPatrol 2506, a vessel similar to the RWS 71 in several operating conditions. These measurements serve as a first estimate of the shaft power demand. In 2022, MARIN measured the auxiliary power of the RWS 71 operating around Dordrecht (type I) across 15 shifts from May 2nd to May 11th. Every shift, the average and the maximum auxiliary power were recorded. The highest recorded day average was 25 kW. For the extreme scenario, the auxiliary power is assumed to be 25 kW during the entire shift, except when crews are switching. Lastly, since this region regards large open waters and the vessel has to be able to sail in rough waters, a 10% sea state correction in added. The total required energy of an extreme 24-hour shift is calculated in table 3.4.

Table 3.4: An extreme operational scenario in a type II region. The power estimations are based on the RWS 71

Extreme 24 hours:						
	Local operation			Transit		
Operation mode	*- Crew switch - Off-duty*	*- Moored - Refueling - Inspection*	*- Calamity - Lock*	*- Cruising speed - Mobile Inspection (∼20 km/h)*	*Intermediate speed (∼30 km/h)*	*Max speed (∼45 km/h)*
hours	6	1	2	4	6	5
power (kW)	0	25	50	248	730	1183
energy (kWh)	0	25	100	992	4380	5915
				Total per day:	**12553**	**kWh**

Region type III calls for resistance estimations at rather low speeds. However, there are no records of shaft power measurements of the RWS 59, a preference vessel in this region. The RWS 22 and the RWS 82 are the only two similar vessels of which shaft power measurements at relatively low speeds are available. This data runs upwards from 8 kn, which is assumed to be the slow cruising speed. The RWS 59 is equipped with an Onan 7 MDKBL, which has a power of 7 kW. The auxiliary power is assumed to be a continuous 7 kW, except when crews are switching or the vessel is off duty. Table 3.5 provides the total required energy in an extreme 16-hour day.

Table 3.5: An extreme operational scenario in a type III region. The power estimations are based on the RWS 59.

Extreme 24 hours:						
	Local operation			Transit		
Operation mode	*- Crew switch* *- Off-duty*	*- Moored* *- Refueling* *- Inspection*	*- Calamity* *- Lock*	*- Cruising speed* *- Mobile Inspection* *(∼10 km/h)*	*Intermediate speed (∼15 km/h)*	*Max speed (∼20 km/h)*
hours	12	1	1	4	3	3
power (kW)	0	7	32	63	144	588
energy (kWh)	0	7	32	252	432	1764
				Total per day:	**2487**	**kWh**

4

Weight & size of the power plant

The resistance of planing hulls depends for a great deal on the weight and size of the vessel. The weight of the zero-emission designs is estimated by calculating the weight difference between the current power plants and the new zero-emission power plants, and adding this difference to the current vessel weight. An increase in the vessel weight induces an increase in resistance, thus increasing the required power and in turn the power plant weight. To enable quick iteration steps in the design phase, a parametric calculation model is developed to make a quick estimate of the total weight and size of the power plant as a function of the required power.

This chapter is structured as follows: in paragraph 4.1, the weight of a current diesel power plant is estimated. Then, in paragraph 4.2, five power plant configurations are introduced, that are to be analysed for each region type. Next, in paragraph 4.3 the weights and sizes of all power plant elements with an alternative energy carrier are estimated. Finally, in paragraph 4.4, the total power plant weight and size are presented as a function of the installed power.

4.1. Size and weight of a current power plant

In 2023, MARIN researched the possibilities of the use of liquid hydrogen as an energy carrier for RWS patrol vessels. To assess the weight change in the vessel with a new energy carrier, they first estimated the weight and size of a power plant in an operating vessel, and the weight and size of the elements associated to a plant powered by an alternative fuel. The operating reference vessel has an installed power of 1360 kW, and the total size and weight of the power plant were estimated to be 12.7 t. This includes two diesel engines, two gearboxes, a generator, 2200 kg of diesel, lubricating oil, the AC distribution, cooling and auxiliary pumps and the exhaust and SCR system (MARIN, personal communication, June 20, 2024).

4.2. Five power plant configurations

RWS considers batteries, hydrogen and methanol to adopt as their a new energy carrier for the patrol fleet. 5 different energy configurations are considered in this research. In the following paragraphs, the total required energy storage capacity is determined for each configuration, based on the extreme operational scenarios set in paragraph 3.2. Initial results of these calculations are shown in table A.1 in appendix A.

4.2.1. Battery electric

RWS's first preference is a battery electric configuration, since it is considered to be climate neutral as well as emission free, as discussed in paragraph 2.1.3. An operational advantage of batteries is that they can be charged during every crew switch, which means that one charge only has to last one shift. However, the total energy demand over 24 hours ($E_{req,24h}$), set in paragraph 3.2, is not evenly distributed over the entire 24 hours of a day. This means that the extreme operational energy demand $E_{req,8h}$ is higher than a third of $E_{req,24h}$. An increase in bunker frequency therefore means a larger

difference between the operational maxima and minima in between every occasion on which a vessel is refueled, since the extremes are averaged out over a smaller time step interval. An energy correction $c_{time\ step}$ is included to account for this asymmetry across different shifts within the same 24 hours. This is a measure of how much more energy is used in one shift compared to another within the same 24 hours. $c_{time\ step}$ influences the maximum time that a vessel can sail at full speed, and its value is chosen according the expected required maximum time spent at full speed.

Several efficiencies inherent to battery storage have to be taken into account. First, batteries have a limited recommended depth of discharge (DoD). This means that the state of charge (SoC) must always stay between set limits to prevent fast degeneration (Park et al., 2023). This DoD differs from battery to battery, depending on the type of chemical components used. Many manufacturers offer batteries for maritime applications on the market. Table 4.1 shows an overview of some of them, with important characteristics. Some manufacturers do not recommend a specific DoD limit to maintain battery life. In those cases the DoD limit is based on the recommendation of a manufacturer of a similar battery.

Table 4.1: An overview of available battery packs for maritime applications.

Battery pack	Producer	Capacity (kWh)	Weight (kg)	Volume (l)	Energy ρ (kWh/kg)	Max DoD	Battery Type
MG LFP [1]	MG	7.8	54	38.87	0.144	80%	LFP
Dolphin NxtGen ESS-Energy [2]	Corvus	8.2	45.5	33.30	0.180	80%[3]	NCA
Octopus High Energy [4]	Est-Floattech	10	86.5	102.33	0.116	80%[3]	NMC
Octopus High Power [4]	Est-Floattech	5.8	82	102.33	0.071	80%[3]	NMC
Aries+ s [5]	AYK	17.6	130	82.72	0.135	100%	LFP
Aquarius+ [5]	AYK	21.5	170	106.93	0.126	100%	LFP
Kaptein Navigator [6]	Tesvolt Ocean	23.5	110	71.50	0.214	80%	NMC

Of all considered batteries, Kaptein Navigator by Tesvolt Ocean has the highest gravimetric energy density, even when taking its DoD limit into account. Therefore, Kaptein Navigator, shown in figure 4.1, is used as the battery reference model for this research. The correction for the DoD limit η_{DoD}, given in table 4.1, is thus equal to 80%.

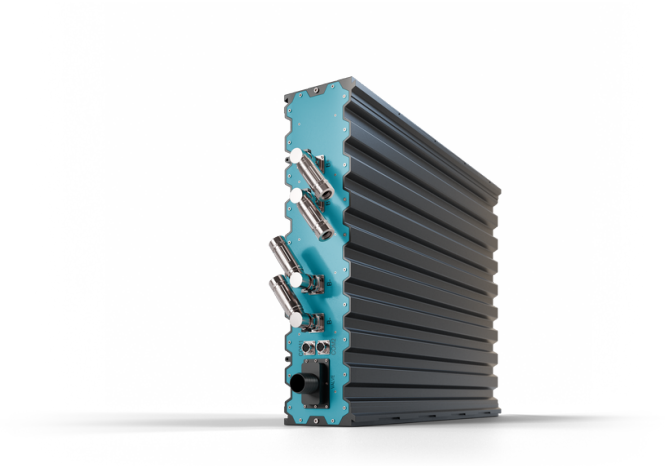

Figure 4.1: Kaptein Navigator battery by Tesvolt Ocean (Tesvolt Ocean, n.d.-b)

[1](MG, 2025)
[2](Corvus Energy, n.d.-a)
[3]Estimated based on the Kaptein Navigator battery
[4](EST-floattech, n.d.)
[5](AYK, n.d.)
[6](Tesvolt Ocean, n.d.-a)

Next, an energy margin of 10% is added to the total amount of required energy to prevent the vessel from depleting its entire energy storage just before reaching the charging station. This 10% energy margin for batteries coincides with the lower end of the DoD limit.

Battery degradation is another factor to take into account. As a battery goes through more cycles, the state of health (SoH) of a battery decreases. Or in other words, the energy a battery can store in a full charge decreases. To anticipate on this effect, more batteries have to be installed in a new ship than strictly necessary, to ensure enough energy can still be stored when the batteries have degraded for a certain percentage over time. For this research, a 10% SoH correction is included.

The coulombic efficiency, converter efficiency and the efficiency of the electrical motor and drive are combined in electrical efficiency $\eta_{batt,electrical}$ (Battery University, 2021; Emrax, n.d.; Zekalabs, n.d.). Finally, transmission efficiency $\eta_{transmission}$ is assumed to be 0.96.

From these efficiencies follows the total battery efficiency:

$$\eta_{batt} = \eta_{DoD} \cdot \eta_{SoH} \cdot \eta_{batt,electrical} \cdot \eta_{transmission} = 80\% \cdot 90\% \cdot 92\% \cdot 96\% = 64\%$$

With the recharging frequency, required energy and battery efficiency, the total required energy storage is calculated:

$$E_{stored,batt} = r_{batt} \cdot E_{req,24h} \cdot t_{refill,batt} \cdot (1 + c_{margin} + c_{time\,step}) \cdot \frac{1}{\eta_{batt}}$$

Next, the total number of batteries is calculated by dividing the required energy storage by the reported gross capacity of the Kaptein Navigator battery, and rounding this up. The gross capacity of one battery is equal to 23.5 kWh, and the net capacity is 18.9 kWh when considering a max SoC of 80%. This 80% has been included when calculating the battery storage efficiency η_{batt}, and is therefore already accounted for in $E_{stored,batt}$.

It is important to note that the required stored energy expressed in kWh exceeds the maximum required power expressed in kW by a ratio of more than 3 to 1. Next to this, the battery with the lowest continuous C-rate of 0.35 is the Aquarius+ produced by AYK, which means that its maximum capacity in kWh exceeds its power in kW by a ratio of 1 to 0.35 (or 2.86 to 1). From this, it is concluded that energy capacity, rather than power, is the limiting factor. Through this research, the battery plant size is thus determined by the required capacity of the batteries, and not the required power.

4.2.2. Battery-fuel cell hybrid

The second energy configuration is an electric hybrid of hydrogen (H_2) fuel cells and batteries. Unlike batteries, hydrogen can not be bunkered from a truck in between every shift, except if the on-board storage tanks can be swapped with full ones stored at berth locations. However, for this thesis, operation with one set of tanks is analysed, because not all vessels always berth in the same harbour, and tanks stored on shore may already be used by another vessel at the same berth location. In consultation with RWS, it is concluded that the minimal time between bunkers in the most extreme case is 2 days, while the average bunker frequency will be lower. In current pilot projects of hydrogen powered vessels of the RWS, hydrogen is brought to the vessel in a hydrogen truck, pressurised at 350 bar. Therefore, hydrogen is assumed to be stored in pressurised tanks at 350 bar. Hydrogen fed proton exchange membrane fuel cells (PEMFC) are used to generate power. In table 4.2 an overview is shown of PEMFCs that are currently available on the market for maritime applications.

Table 4.2: An overview of available PEMFCs for maritime applications

PEMFC	Producer	Power (kW)	Weight (kg)	Volume (l)	Power ρ (kW/l)	Power ρ (kW/kg)	Efficiency
HyPM HD 180 [7]	Hydrogenics	198	654	1005	0.20	0.30	0.55
FC Wave [8]	Ballard	200	1000	1966	0.10	0.20	0.54
Pelican FC [9]	Corvus	340	3750	7151	0.05	0.09	N/A
Horizon VL-120 [10]	Horizon	120	290	514	0.23	0.41	0.48
Marine System 225 [11]	Powercell	225	1000	2160	0.10	0.23	0.56
zepp.X150 [12]	zepp.solutions	150	355	595	0.25	0.42	0.57

Zepp.X150 has both the highest gravimetric and volumetric power density. Therefore, for the rest of this research, the specifications of this PEMFC, shown in figure 4.2, will be used as the reference for calculations regarding PEMFCs. The efficiency of this fuel cell at 50% of its rated power is 57% of the lower heating value of hydrogen, and at its rated power output, the efficiency drops to 51%.

Figure 4.2: zepp.X150 by zepp.solutions (zepp.solutions, n.d.)

The extreme scenarios in tables 3.3, 3.4 and 3.5 show that most energy will be used in operating modes with relatively high power demands. Therefore, the chemical output efficiency of the fuel cells, $\eta_{FC,output}$, is estimated to be 54%. The electrical efficiency of the fuel cell is equal to that of batteries excluding the coulombic efficiency of 99%. Thus, $\eta_{FC,electrical}$ is assumed to be 93%. And analogous to batteries, the transmission efficiency $\eta_{transmission}$ is estimated to be 96%. This gives a total efficiency of:

$$\eta_{PEMFC} = \eta_{FC,output} \cdot \eta_{FC,electrical} \cdot \eta_{transmission} = 54\% \cdot 93\% \cdot 96\% = 48\%$$

The bunker and recharging frequency are now set, as well as the efficiency of both energy carriers. Next, the ratio of hydrogen storage energy to battery storage energy must be established. This ratio is paramount to calculate the weight and size of the power plant. To enable adjustments later on in the

[7](Hydrogenics, n.d.)
[8](Ballard, 2024)
[9](Corvus Energy, n.d.-b)
[10](Horizon Educational, n.d.)
[11](PowerCell, n.d.)
[12](zepp.solutions, n.d.)

design process, a parametric calculation is defined to determine the total required energy storage of both energy carriers as a function of this energy ratio.

First, the ratios of energy capacity of both carriers (as a percentage of $E_{req,24h}$) are defined as input variables r_{H_2} and r_{batt}. Then, these ratios are multiplied with $E_{req,24h}$ and the time between bunkers of the energy carriers t_{refill,H_2} and $t_{refill,batt}$.

Similar to batteries, hydrogen also has a fuel margin c_{margin} of 10% added to the required capacity to prevent depletion just before reaching the bunker station. And for batteries in the hybrid configuration, $c_{time\ step}$ of 30% is again included. In formula form, the total required energy storage capacity is calculated as follows, with $r_{batt} + r_{H_2} = 1$:

$$E_{stored,H_2} = r_{H_2} \cdot E_{req,24h} \cdot t_{refill,H_2} \cdot (1 + c_{margin}) \cdot \frac{1}{\eta_{PEMFC}}$$

Next, the required installed fuel cell power (P_{FC}) is determined by multiplying r_{H_2} with the total required installed power. One Zepp.X150 PEMFC has a maximum power output of 150 kW. The amount of fuel cells is equal to P_{FC} divided by 150 kW, rounded up. The amount of batteries is calculated by dividing $E_{stored,batt}$ by the energy capacity of the Kaptein Navigator capacity, which is 23.5 kWh.

4.2.3. Hydrogen powered internal combustion engine

The third power generator considered is an internal combustion engine (ICE) powered with hydrogen. Like in the case of the battery-hydrogen hybrid, the minimal time between bunkers is again 2 days and a fuel margin of 10% is included. Regarding the fuel efficiency of a hydrogen ICE: the X15H by Cummins (Buckley, 2023) and the MAN H4576 (Van den Meer, I., 2023) both have a maximum efficiency of 45%. The MAN H4576 is shown in figure 4.3.

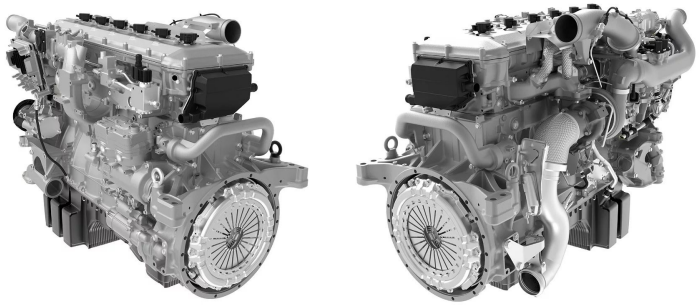

Figure 4.3: The hydrogen powered MAN H4576 internal combustion engine (MAN Engines, n.d.)

Taking into account that the engine is not expected to run at the ideal operating point under ideal conditions, the average fuel efficiency of a hydrogen ICE is assumed to be 41%. The transmission efficiency is 96%. From this follows:

$$\eta_{H_2\,ICE} = 41\% \cdot 96\% = 39\%$$

The total required energy storage of hydrogen in this configuration is subsequently determined:

$$E_{stored,H_2} = E_{req,24h} \cdot t_{refill,H_2} \cdot (1 + c_{margin}) \cdot \frac{1}{\eta_{H_2\,ICE}}$$

The installed power of the engine is equal to the total required power that is defined in paragraph 3.2. The maximum time that can be spent in each of the operating modes is calculated by dividing the power demand of the modes by E_{prop}.

4.2.4. Methanol powered internal combustion engine

The fourth considered energy configuration encompasses a methanol, or CH_3OH, fed internal combustion engine. The availability of methanol engines with an installed power between 450 kW and 1000 kW on the market is limited. The MD97 produced by ScandiNAOS has a maximum power of 450 kW (ScandiNAOS AB, n.d.). It is shown in figure 4.4.

Figure 4.4: The methanol-powered MD97 by ScandiaNAOS (ScandiNAOS AB, n.d.)

This engine is used as a reference for the efficiency of a methanol engine. Through personal communication to RWS, it is concluded that a typical methanol engine in this power range has a specific energy consumption of 470 g/kWh. Methanol has a lower heating value of 5.53 kWh/kg (Methanol Institute, n.d.-a), which is equivalent to 181 g/kWh. Thus, a methanol engines' fuel efficiency is assumed to be $\frac{181}{470}$ or 38.5%. The fuel margin and transmission efficiency are equal to the hydrogen fed ICE configuration, which are respectively 10% and 96%. The efficiency and required energy storage are calculated similarly:

$$\eta_{CH_3OH\,ICE} = 38.5\% \cdot 96\% = 37\%$$

$$E_{stored,CH_3OH} = E_{req,24h} \cdot t_{refill,CH_3OH} \cdot (1 + c_{margin}) \cdot \frac{1}{\eta_{CH_3OH\,ICE}}$$

A limitation of methanol usage is the power range of methanol engines that are available on the market. ScandiNAOS AB (n.d.) offers methanol engines in the range of 150 kW to 450 kW.

4.2.5. Battery-methanol hybrid

The last energy configuration that is considered is a methanol-electric hybrid. This hybrid is analysed, because batteries are preferred by the RWS, while it is expected that methanol will have the most energy dense power and storage plant of the three energy carriers. For methanol, an ICE will be used to generate power. However, the chemical energy stored in the batteries will be used to power an electric motor. The HP Inline parallel hybrid propulsion system by Hydrosta enables both an electrical motor and an ICE to drive one shaft (Hydrosta, n.d.). The electrical motors used on the shaft are axial flux motors produced by Phi Power. The outer diameter of the Ph381 and Ph382, their strongest motors, is 380 mm (Phi-power, n.d.). This is assumed to be the outer diameter of the HP Inline system. With the length of the system reported by Hydrosta, the total size is configurated. In table 4.3 the specifications of the HP Inline are shown. In each configuration, the maximum installed methanol engine power can not exceed 1200 kW, while the size and weight of the electrical motor depends on the maximum chosen installed electrical power.

Table 4.3: The weight and size of the HP Inline system that allows for a ICE-electric hybrid on the same shaft

Maximum engine power (kW)	Maximum electrical power (kW)	HP Inline weight (kg)	HP Inline size (m3)
1200	180	420	0.058
1200	360	560	0.072
1200	540	700	0.086

Similar to the battery-fuel cell hybrid, the ratios r_{CH_3OH} and r_{batt} in which the energy is distributed over both carriers must be chosen. This ratio will be chosen to optimise for the plant size and weight, both of which will be estimated in paragraph 4.4.

Again, $t_{refill,batt}$ and t_{refill,CH_3OH} are respectively 8 hours and 2 days, $c_{time\,step}$ for batteries is 30%, both fuels have a c_{margin} of 10%, and η_{batt} and $\eta_{CH_3OH\,ICE}$ are respectively 64% and 37%.

4.3. Energy storage and power generation elements

To estimate the total mass and size of the power plant, an overview is made of elements that are in the current power plant, as well as elements that are to be added in each power configuration. The volumes of the components are calculated by multiplying the dimensions of the outer boundaries, unless otherwise stated.

4.3.1. Energy storage

First, the weight and size of the energy storage units must be calculated. The reference battery for this research is the Kaptein Navigator (Tesvolt Ocean, n.d.-a), because of its relatively high energy density as shown in table 4.1. Multiplying the weight of one battery by the amount of batteries, and adding the weight of a power distribution unit per 7 batteries as reported by Tesvolt, gives the total battery weight. The size is calculated analogously using the reported dimensions.

In the case of hydrogen, the storage weight depends on the amount of pressurised tanks needed. The H2-35-450X2126, a hydrogen tank produced by Hexagon Purus, is used as a reference tank for this research. A 350 bar tank is preferred over a 700 bar tank, because of their higher energy capacity to weight ratio (Hexagon Purus, 2025). A type 4 hydrogen tank is selected, because compared to types 1, 2 and 3, it has the highest energy capacity relative to its total weight (AlZohbi et al., 2023; Li et al., 2024). For the distribution of hydrogen throughout the vessel, MARIN assumes the total additional weight needed for piping and valves, compared to a diesel installation, is 220 kg. Additionally, a 400 kg bunker station on deck is required to safely transfer the pressurised hydrogen from on-shore facility to the tanks. This includes a cabinet with double walled pipes leading to the tanks, coupling equipment for the bunker hose, and a control & monitoring system. After further inquiry with MARIN, it is concluded that some of these system can be simplified and located on-shore. Because of this, it is assumed 200 kg must be added to the power plant weight, as opposed to 400 kg (MARIN, personal communication, June 20, 2024).

The weight and volume of the stored methanol is calculated using the energy density of methanol, which is 19.9 kJ/g, or 5.53 kWh/kg, and the gravimetric density which is 0.79 kg/l (Methanol Institute, n.d.-a). From this follows that the volumetric energy density is 4.98 kWh/l. These densities are multiplied by E_{stored,CH_3OH} in kWh to find the total weight and volume of the methanol.

Apart from the methanol itself, additional material around the tanks will be needed to meet the safety requirements imposed by class societies. According to section 3.1.2.2 of Bureau Veritas' rules regarding methanol and ethanol-fuelled ships: 'Integral fuel tanks are to be surrounded by protective cofferdams, except on those surfaces bound by shell plating below the lowest possible waterline, other fuel tanks containing methyl/ethyl alcohol, or fuel preparation space' (Bureau Veritas, 2024). This is depicted in figure 4.5.

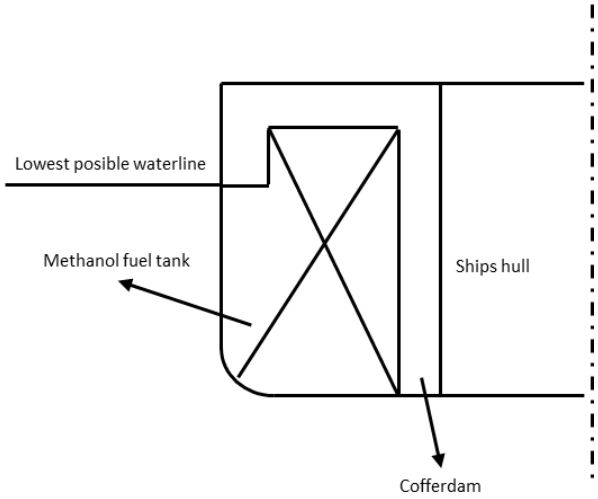

Figure 4.5: The required placement of cofferdams around methanol storage tanks (Marine Service Noord, n.d.)

If methanol is stored in the double hull and bottom under the lowest waterline, then extra material is needed for three double-walled tank boundaries: one in front of the methanol tank, one aft of the methanol tank, and one on top of the tank. Assuming the ends of the methanol tanks coincide with two transverse bulkheads, two extra plates are needed to create the cofferdam spaces aft and in front of the tanks. According to Pt. B, Ch. 2, Sec. 2, par. 3.1.2, the minimal height of the double bottom is not to be less than 0.76 m (Bureau Veritas, 2025b). The height of the bulkheads is estimated at 0.8 m. The width will be approximately equal to the vessels' beam, and is estimated at 5.5 m. The plate thickness of the cofferdams is estimated at 0.3 cm, since these cofferdams are designed to hold inert gas and are added to a construction that is already sufficiently strong. The rounded bilge is assumed to deduct 30% of the total area of the bulkheads. Stiffening is assumed to add 20% to the total plate weight. The construction material of the RWS 70-series vessels is steel with a density of 7850 kg/m^3 (The Engineering Toolbox, 2004), and the construction material of the RWS 21 is aluminium with a density of 2710 kg/m^3 (Thyssenkrupp, 2023). It is assumed that the cofferdams are made out of the same material as the main construction material of each vessel.

4.3.2. Power generators

As for the power generation, three different power generator types are considered: batteries, fuel cells and internal combustion engines (ICEs). The weight and size calculations of batteries have been explained in paragraph 4.3.1. For every 200 kW of required battery power, the weight and volume of an additional DC-DC converter are included. The RedPrime 200 kW DC-DC converter is taken as a reference for an example of a converter, with a weight of 30 kg and a volume of 40 l (Zekalabs, n.d.).

For hydrogen, fuel cells and an ICE are considered. The reference fuel cell for this research is the zepp.X150, which is selected in paragraph 4.2.2. One zepp.X150 weighs 355 kg and has a volume of about 0.6 m^3. And for each individual fuel cell, the additional weight and size of a DC-DC converter are included, similar to batteries.

The weight and size of an H_2 ICE are estimated based on the MAN H4576, with a power of 368 kW. Its design is based on the design of the established MAN D3876, a diesel engine with a power of up to 485 kW. MAN reports 80% of its parts are the same, and the dimensions are 'almost identical' (MAN Engines, 2023). Assuming the engines both have approximately the same weight and size, the power density of a MAN hydrogen engine is 25% lower than that of a regular diesel engine. Thus, the weight of a hydrogen engine is assumed to be around 125% of that of a regular diesel engine, and the size is assumed to be the same. A list of diesel engines used as a reference for this research is presented in appendix C. Essential for the functioning of an internal combustion engine is lubricating oil. MARIN reports a lubricating oil weight of 200 kg, with a tank volume of 160 l. These are added in the configurations using an ICE.

To operate an internal combustion engine, exhaust gas after-treatment is necessary. In the Sustainable Power Database published by MARIN, an average exhaust and after-treatment installation weight of 1.25 kg/kW of installed power is reported, and a volume of 5.12 l/kW (MARIN, 2020). These average values are used as an indication of the exhaust system weight and size.

4.3.3. Power electronics

In the case of an electrical power plant, power will be transferred to the propeller by an electric motor. First, axial flux motors are considered, for they are lighter and smaller than radial flux motors. A selection of available axial flux motors is shown in appendix C in table C.1. However, the maximum power that axial flux motors can deliver continuously is limited. In case the power of the axial flux motor is insufficient, the weight and size of a heavier radial flux motor with a rated power corresponding with the required installed power is used as a reference.

In an electrical power plant, the distribution of the electrical power delivered by the batteries and fuel cells must be controlled. The drive and electric motor run on direct current, while several on-board systems, like pumps and lights, run on alternating current. Therefore, electronic equipment is needed to manage the DC distribution and AC distribution. MARIN and Mauric, a French engineering company, have reported estimations of the weights and sizes of the necessary components. These are used as a reference (MARIN, personal communication, June 20, 2024).

The two main components in the electronic equipment are the DC and AC distribution itself. These are connected by two (for redundancy) grid converters. Two converters are also needed to connect the AC fed electric motors on the shaft to the DC distribution. The converters and distribution systems are placed in designated electrical cabinets, to protect them from water and dust. For a vessel with a maximum combined electric motor power of 1166 kW, Mauric estimated the combined weight of these electrical components to be 2001 kg.

For the purpose of this research, it is assumed that the weight of the aforementioned electrical components is scaled linearly with the total required electric motor power, with 2001 kg at 1166 kW as a reference point.

4.3.4. Cooling circuits

Finally, the weight of the cooling system must also be accounted for. MARIN estimated the total cooling system weight to be 2191 kg, divided between 3 circuits: a closed medium temperature circuit to cool the electrical components like drives and converters, a closed low temperature circuit to cool batteries, and a raw water circuit, which is used to cool the fuel cells and to which the other two circuits give off their heat (MARIN, personal communication, June 20, 2024).

In consultation with MARIN, the assumption is made that the total cooling system weight is scaled linearly with the installed power, which in the MARIN estimation was a power of 1360 kW. Even though every power configuration uses different power generation methods, and thus might need different configurations of cooling circuits, they all require to lose heat in order to function properly and safely. And with every power generation method, an increase in total installed power requires an increase total installed cooling power.

4.3.5. Nitrogen, transmission and insulation

To store methanol, an inerting system is required. According to sec. 4, par. 5.1 of Bureau Veritas rules regarding methanol and ethanol fuelled ships, ‘Inert gas should be available permanently on board in order to achieve at least one trip from port to port considering maximum consumption of fuel expected and maximum length of trip expected and to keep tanks inerted during two weeks in harbour with minimum port consumption’, and ‘A production plant and/or adequate storage capacities might be used to achieve [previously mentioned] availability target’ (Bureau Veritas, 2024). Through personal inquiry with MARIN, the Maxigas MX104 is deemed to be sufficient for the on-board production of nitrogen without the need for additional nitrogen tanks as a supply buffer. This nitrogen generator weighs 336 kg (Manualslib, n.d.). MARIN estimates the required volume for such a system to be 0.72 m^3. The distribution of the nitrogen to the tanks requires some additional weight for pipes and valves, with an estimated weight of 30% of the Maxigas MX104 generator.

Next, most electric motors considered for this research have a maximum speed between 1500 and 2000 rpm, while the maximum speed of the heavy duty internal combustion engines by MAN is 1600

rpm. The propeller speed is typically lower. A gearbox must therefore also be included. ZF offers gearboxes in the power and speed range of the engines and motors. The ZF 665 has an input power capacity of 559 kW at a speed of 1800 rpm, with a transmission ratio between 1.1 and 2 (ZF, n.d.). This gearbox is therefore used as a reference. The dry weight is 248 kg, with an additional oil weight of 16 l. Assuming lubricating oil has a density of 0.85 kg/l (Lubex, 2023), this adds another 14 kg. Thus, the total gearbox weight per electric machine or engine is assumed to be 262 kg.

Next, Bureau Veritas prescribes A-60 insulation is needed in category A spaces. In the case of patrol vessels powered by alternative fuels, this applies to the fuel cell rooms and battery storage rooms. To estimate the weight of the insulation material, the outside area of the rooms is needed. To approximate the outside area of battery and fuel cell room as a function of the amount of batteries or cells inside, basic layouts of multiple battery and fuel cell rooms are sketched.

First, the size of one wall of Kaptein Navigator batteries is determined, including an additional 20 cm behind the wall for cooling equipment and a meter of space in front of the wall to allow for maintenance work. Adding another wall will increase the depth of the room by the depth of one battery plus the additional cooling space of 20 cm, which is 0.97 m. When a third wall is added, the depth of the room increases by the depth of another wall and cooling equipment, but also another meter of maintenance space. This is shown in figure 4.6.

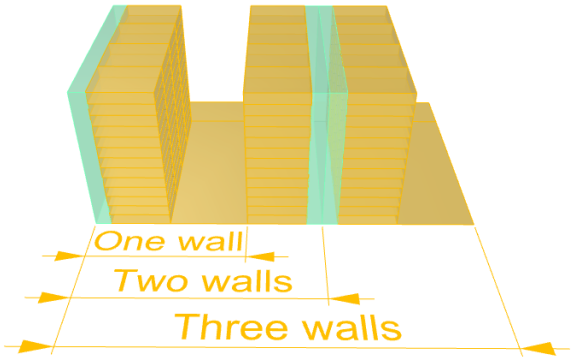

Figure 4.6: Dependency of battery room size on amount of battery walls. The batteries are depicted in orange, with the blue parts being space reserved for cooling. Between the walls, a floor area is reserved for maintenance.

The total number of walls is equal to the amount of required batteries $\#_{batt}$ divided by the amount of batteries that fits in a wall, which is chosen to be 48. One wall is 11 batteries or 1.79 m high, and has width of 3.1 m, which is the width of 4 batteries and has a 60 cm space next to the batteries to make all walls reachable. This way, the depth of the room L of the room can be calculated:

$$L = \frac{\#_{batt}}{52} \cdot 0.97m + \left\lceil \frac{1}{2} \cdot \frac{\#_{batt}}{48} \right\rceil \cdot 1m$$

The lightest Isover insulation material for aluminium ships is used as a reference for the insulation weight. The bulkhead insulation weighs 10.69 kg/m^2 (Isover Saint-Gobain, n.d.-a), and the deck insulation weighs 7.85 kg/m^2 (Isover Saint-Gobain, n.d.-b). The estimated weights for the insulation material are shown in table 4.4.

Table 4.4: The weight of the required insulation material in a battery storage room

Number of walls	Insulation mass (kg)
1	224
2	288
3	418
4	481
5	611

The area of the outer boundaries of the fuel cell room are determined in a similar fashion. In 3D drawing software, the outer boundary area is measured of a fuel cell room containing up to 8 fuel cells. Through personal inquiry with zepp.solutions, it is confirmed that the fuel cells are stackable in all directions. 3 different fuel cell room sizes are designed, with a capacity of up to 2, 4 and 8 fuel cells, shown in figure 4.7.

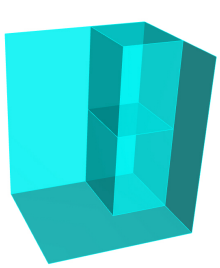

(a) Fuel cell room with a capacity of up to 2 zepp.X150s

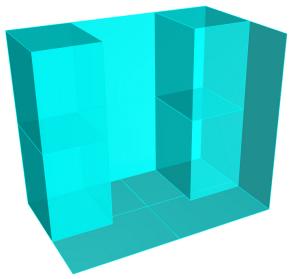

(b) Fuel cell room with a capacity of up to 4 zepp.X150s

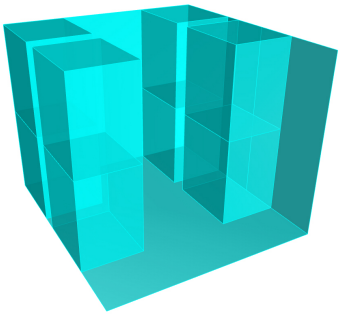

(c) Fuel cell room with a capacity of up to 8 zepp.X150s

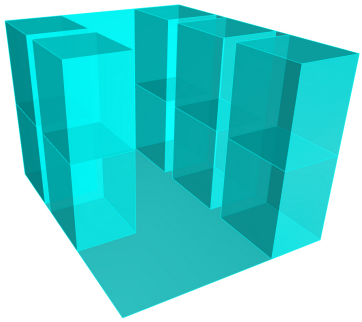

(d) Fuel cell room with a capacity of up to 10 zepp.X150s

Figure 4.7: Four sizes of fuel cell room

Using the Isover insulation material weights, the insulation weight estimations as a function of the total number of installed fuel cells are shown in table 4.5.

Table 4.5: The weight of the required insulation material in a fuel cell room

Number of fuel cells	Insulation mass (kg)
1	174
2	174
3	193
4	193
5	305
6	305
7	305
8	305
9	342
10	342

4.4. Total power plant weight & size

The previous paragraph explains how P_{req} is used to estimate the weight and size of the most important power plant elements. The weight and size of the entire power plant is found by adding the weights and volumes of all individual elements. In table 4.6 the cumulative results are shown. In table A.1 in appendix A, the the estimations of all elements of a power plant with an alternative energy carrier are shown for the the original vessels operating in a type I, type II and type II region.

Table 4.6: Cumulative non-hybrid power plant weights and sizes in each of the region types

	Battery electric		**H2 ICE**		**Methanol ICE**	
	Weight (t)	Size (m3)	Weight (t)	Size (m3)	Weight (t)	Size (m3)
Region type I	31.0	25.5	23.5	87.0	15.0	24.4
Region type II	50.0	39.5	35.9	141.5	21.0	34.2
Region type III	8.3	7.2	9.0	23.9	6.7	10.6

For the hybrid configurations, the total weight and size of the power plant also depends on the energy carrier capacity ratios. The optimal values of these ratios have yet to be determined. To select the optimal ratio, r_{batt} and r_{H_2} or r_{CH_3OH} are varied between 0.1 and 0.9, and for each variation the sum of the weight and volume of all discussed power plant elements is recorded.

Figure 4.8a shows the cumulative weight and size of all components in a battery-fuel cell hybrid in a region of type I. These results show that as more energy is stored in the form of hydrogen, the entire power plant becomes almost linearly lighter, but more voluminous. Figure 4.8b shows that the power plant becomes almost linearly heavier and larger as more energy is stored in the form of batteries instead of methanol.

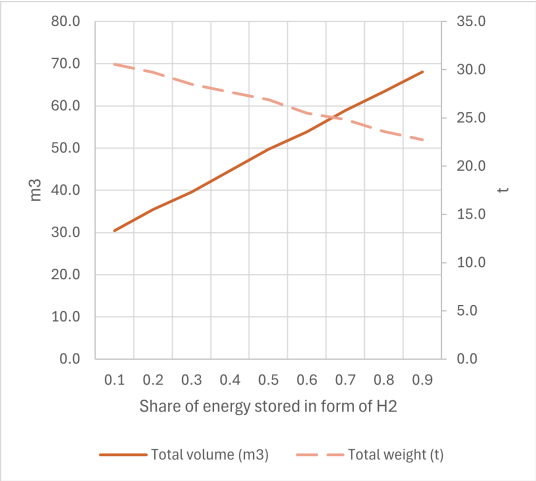

(a) The total power plant weight and size as a function of r_{H_2} in the battery-fuel cell hybrid configuration

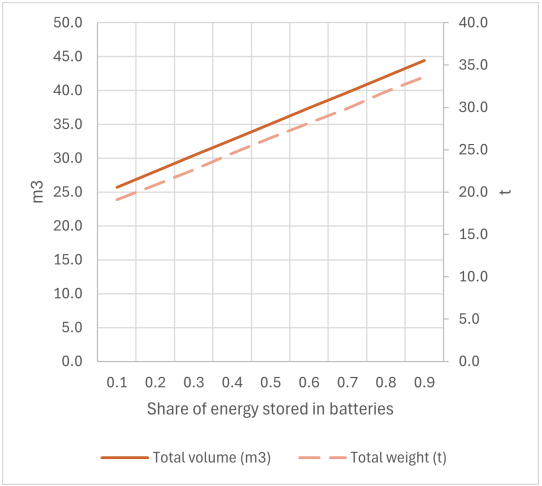

(b) The total power plant weight and size as a function of r_{batt} in the battery-methanol ICE hybrid configuration

Figure 4.8: The dependency of power plant weight and size on the fuel ratios in hybrid systems in region type I

Similar to the results of region I, figure 4.9a shows that the power plant becomes larger, but lighter as more energy is stored in the form of compressed hydrogen. And figure 4.9b shows an almost linear relationship between the share of energy stored in the form of methanol and the power plant's weight and size. As a result of the larger energy storage requirement, the total mass and volume are higher than in a type I region.

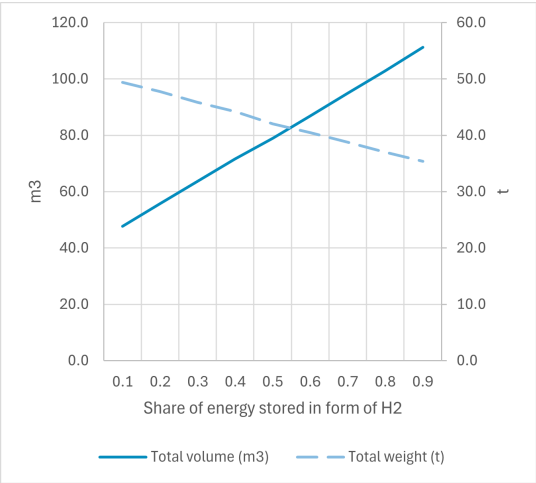

(a) The total power plant weight and size as a function of r_{H_2} in the battery-fuel cell hybrid configuration

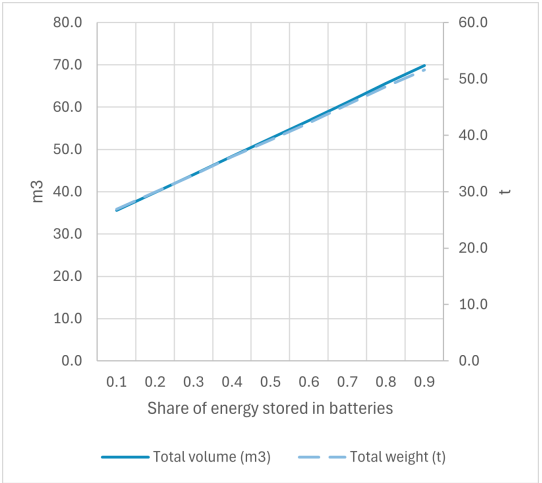

(b) The total power plant weight and size as a function of r_{batt} in the battery-methanol ICE hybrid configuration

Figure 4.9: The dependency of power plant weight and size on the fuel ratios in hybrid systems in region type II

Figures 4.10a and 4.10b show results the results of hybrid power plant weights and sizes, which are similar to region types I and II. At a fuel ratio of 0.5 and 0.6, the graphs show a nod. At this fuel ratio, the power plant switches from one to two fuel cells. Because the installed power of this power plant is lower than region types I and II, it is more sensitive to changes like the addition of a fuel cell.

(a) The total power plant weight and size as a function of r_{H_2} in the battery-fuel cell hybrid configuration

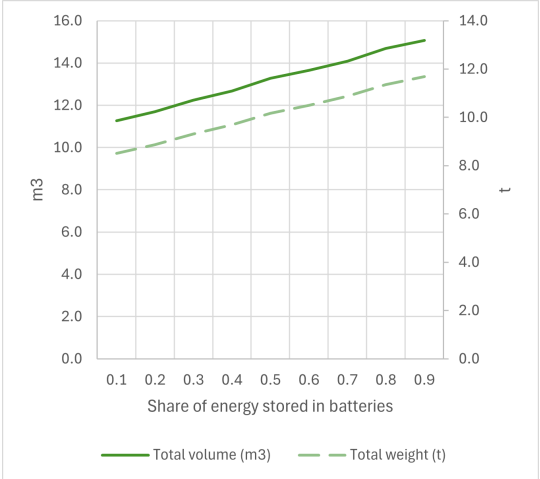

(b) The total power plant weight and size as a function of r_{batt} in the battery-methanol ICE hybrid configuration

Figure 4.10: The dependency of power plant weight and size on the fuel ratios in hybrid systems in region type III

5

Resistance and required power

In the previous chapter, the weight and size of the power plant are estimated as a function of the installed power. In this chapter, a method is designed to predict the required installed power as a function of the ship resistance.

First, in paragraph 5.1 the total ship resistance is calculated for each region type, using the ship parameters of 3D models resembling the actual operating patrol vessels. In paragraph 5.2 the found resistance is used to calculate the required installed power for each vessel, by estimating the propulsive efficiency.

5.1. Resistance prediction

In regions of type I and II, the reference vessels are equipped with a hard chine to enable operation in a semi-displacement mode. The reference vessel in region type III does not operate at high speeds. Therefore, a different resistance prediction

5.1.1. 3D models of reference hulls

To predict the resistance of a vessel like the RWS 21 that is to operate in type I regions, a 3D hull was constructed in Rhinoceros based on a the linesplan of a patrol vessel with a length of 18.8 m, a width of 4.6 m and a draught of 1 m (J. Gelling, personal communication, December 18, 2024). This reference hull is shown in figure 5.1.

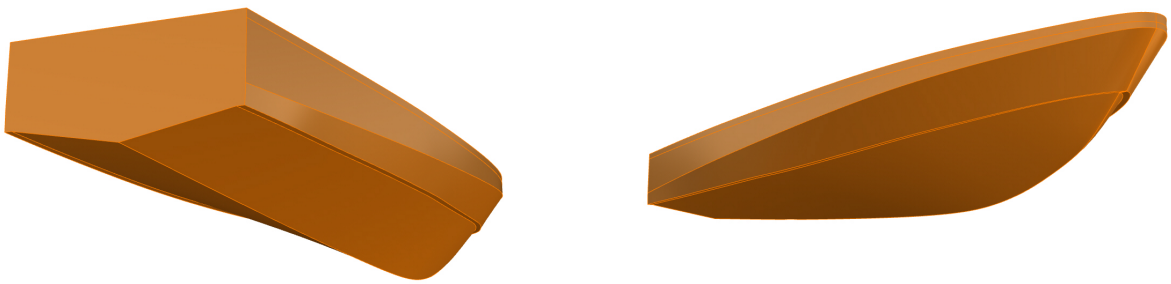

(a) The stern of the model resembling the RWS 21

(b) The bow of the model resembling the RWS 21

Figure 5.1: The 3D model of the RWS 21 reference hull

Like the RWS 21, the RWS 71 is also equipped with a hard chine. A hull resembling the RWS 71 is

constructed by adjusting the hull in figure 5.1 using the ship's main dimensions, dry dock pictures, and the general arrangement drawing of the RWS 71. The resulting model is shown in figure 5.2.

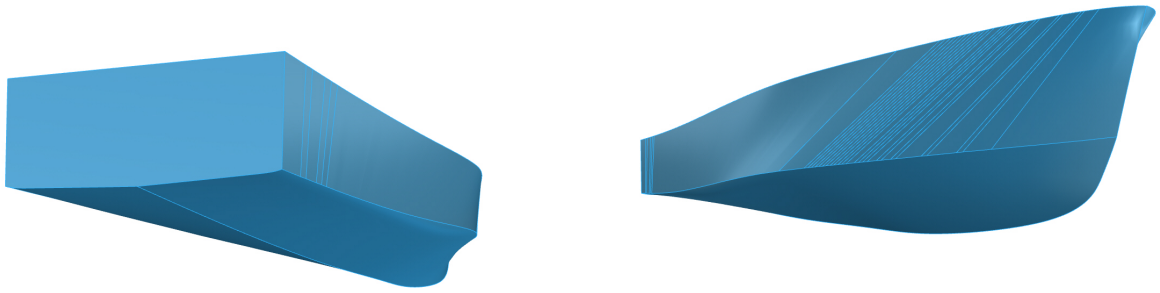

(a) The bow of the model resembling the RWS 71

(b) The stern of the model resembling the RWS 71

Figure 5.2: The 3D model of the RWS 71 reference hull

The last hull to be constructed is the RWS 59. This hull is constructed by using the ship's main dimensions, dry dock pictures and the general arrangement drawing. The constructed hull is shown in figure 5.3.

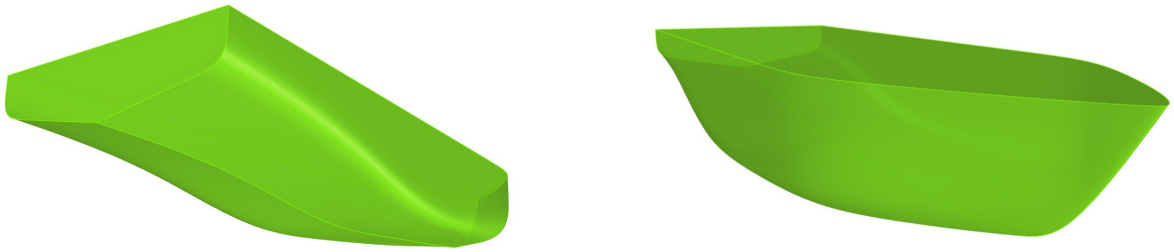

(a) The bow of the reference hull

(b) The stern of the reference hull

Figure 5.3: 3D model resembling the RWS 59

5.1.2. Delft Systematic Deadrise Series

For region types I and II, the Delft Systematic Deadrise Series (DSDS) is used to predict the ship resistance. The calculation in this paragraph follows the steps described by L. Keuning & W. Hillege in 'The results of the Delft Systematic Deadrise Series' (2017). This series is designed for vessels with a displacement Froude number F_∇ between 0.75 and 3.0, and takes into account deadrise, rocker and twist.

Using DSDS, a polynomial expression has been defined to predict the resistance of a prismatic hull.

$$\begin{aligned}\frac{R_t}{\Delta} = a_0 + a_1 LCG + a_2 LCG^2 + a_3\left(\frac{L_p}{B_{px}}\right) + a_4\left(\frac{L_p}{B_{px}}\right)^2 + a_5\left(\frac{L_p}{B_{px}}\right)^3 \\ + a_6\left(\frac{A_p}{\nabla^{\frac{2}{3}}}\right) + a_7\left(\frac{A_p}{\nabla^{\frac{2}{3}}}\right)^2 + a_8\left(\frac{Ap}{\nabla^{\frac{2}{3}}}\right)^3 + a_9\left(LCG \cdot \frac{L_p}{B_{px}}\right) \\ + a_{10}\left(LCG \cdot \frac{A_p}{\nabla^{\frac{2}{3}}}\right) + a_{11}\left(\frac{L_p}{B_{px}} \cdot \frac{A_p}{\nabla^{\frac{2}{3}}}\right)\end{aligned} \tag{5.1}$$

In this expression, R_t is the total ship resistance in N, Δ is the displacement weight of the vessel in kg, L_P is the length of projected planing bottom area between the chines in m, LCG is the longitudinal

center of gravity measured from Ord. 10 as a percentage of L_p, B_{px} is the maximum breadth over the chines in m, and A_p is the projected planing bottom area in m^2. These parameters are measured on the 3D Rhinoceros hull. The longitudinal center of gravity is assumed to be directly above the center of buoyancy in a static condition, since the vessel would start to pitch if this were not the case.

The DSDS database defines a value of a_0 through a_{11} – this set is hereinafter referred to as 'a_{0-11}' – at several values of displacement volume ∇, deadrise angle β and F_∇. These values are shown in table 5.1.

Table 5.1: Values of ∇, β and F_∇ at which a_0 through a_{11} are defined

Parameter	Value at which a-coefficients are defined
$\nabla(m^3)$	2.5, 5, 10, 25, 50, 100, 200, 500, 1000, 2000, 5000
$\beta(°)$	12.5, 19, 25, 30
$F_\nabla(-)$	0.75, 1, 1.25, 1.5, 1.75, 2, 2.25, 2.5, 2.75, 3

Formula 5.2 shows how the displacement Froude number is computed. v_s is the ship's speed in m/s and g is the gravitational constant in m/s^2.

$$Fn_\nabla = \frac{v_s}{\sqrt{g\sqrt[3]{\nabla}}} \quad \Leftrightarrow \quad v_s = Fn_\nabla \cdot \sqrt{g\sqrt[3]{\nabla}} \tag{5.2}$$

Through interpolation, the values of a_{0-11} are found for vessels with displacement volumes and deadrise angles in between the defined data points: first, ∇ and β of the vessel in Rhinoceros are measured, and it is established in between which of the defined entries of ∇ and β given in table 5.1 the values of a_{0-11} must interpolated. This gives values of ∇ and two values of β, and thus four possible combinations of ∇ and β. Next, the values of a_{0-11} at each of the four combinations are extracted from the DSDS database. This gives four sets of a_{0-11}, each of which contains 120 data points (12 a-coefficients for all 10 Froude numbers). The two sets corresponding to the lower β are interpolated linearly between the lower and higher ∇ using the measured ∇ from Rhinoceros. The same is done with the two sets corresponding to the higher β. The resulting sets are used for interpolation between both values of β. Figure 5.4 shows a schematic of the interpolation steps.

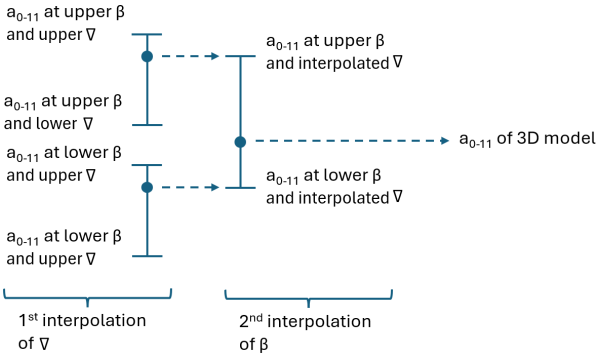

Figure 5.4: Two interpolation steps used to obtain a_{0-11} for a 3D modelled vessel

The final set a_{0-11} is inserted into formula 5.1 once for each Fn_∇. This way, $\frac{R_t}{\Delta}$ is obtained for 10 different Froude numbers for a prismatic hull. However, the hulls of the patrol vessels are not prismatic. The deadrise angle and the depth of the keel vary along the length of the vessel. These characteristics are called twist and rocker respectively. A correction must be applied to the obtained values of $\frac{R_t}{\Delta}$ to account for the twist and rocker. This correction is calculated with another polynomial expression, provided in equation 5.3. In this expression, γ is the average centerline angle from Ord. 10 to Ord. 0

w.r.t. the baseline in °, ε is the deadrise at Ord. 10 minus the deadrise at Ord. 0 in °. The values of these parameters are determined through measurements on the 3D hull.

$$\begin{aligned}\frac{dR_t}{\Delta} = {} & b_0\gamma + b_1\varepsilon + b_2\left(\gamma \cdot \frac{A_p}{\nabla^{\frac{2}{3}}}\right) + b_3\left(\gamma \cdot LCG\right) + b_4\left(\gamma \cdot \frac{L_p}{B_{px}}\right) + b_5\left(\varepsilon \cdot \frac{A_p}{\nabla^{\frac{2}{3}}}\right) \\ & + b_6\left(\varepsilon \cdot LCG\right) + b_7\left(\varepsilon \cdot \frac{L_p}{B_{px}}\right) + b_8\left(\gamma\left(\frac{A_p}{\nabla^{\frac{2}{3}}}\right)^2\right) + b_9\left(\gamma \cdot LCG^2\right) \\ & + b_{10}\left(\gamma \cdot \frac{A_p}{\nabla^{\frac{2}{3}}} \cdot \frac{L_p}{B_{px}}\right) + b_{11}\left(\gamma \cdot \frac{A_p}{\nabla^{\frac{2}{3}}} \cdot LCG\right) + b_{12}\left(\gamma \cdot LCG \cdot \frac{L_p}{B_{px}}\right)\end{aligned} \tag{5.3}$$

Analogous to obtaining a_{0-11}, the set of values of all b-coefficients (b_{0-11}) is obtained by extracting four sets from the DSDS database for b-values, at each combination of ∇ and β directly below and above the measured ∇ and β of the 3D hull. Finally, the sum of $\frac{dR_t}{\Delta}$ and $\frac{dR_t}{\Delta}$ is multiplied by Δ. This way, the total ship resistance R_t is found for vessels in type I and type II regions.

5.1.3. Holtrop & Mennen

For the vessel in region type III, the RWS 59 is used as a reference vessel. In contrast to the RWS 21 and RWS 71, the RWS 59 is a displacement vessel with a U-shaped hull. For the resistance prediction of this vessel, the method developed by Holtrop & Mennen (Holtrop & Mennen, 1982) is applied. This is done by using the online tool provided by The Engineering Handbook (The Engineering Handbook, 2024).

5.2. Propulsive efficiency

The total resistance R_t, obtained in the previous paragraphs, is now to be translated to an effective towing power P_E. By making an estimation of the propulsive efficiency η_D, P_E is used to estimate the required propeller power. η_D encapsulates several efficiencies associated with hydrodynamic interactions of the propeller and hull. These are shown in figure 5.5.

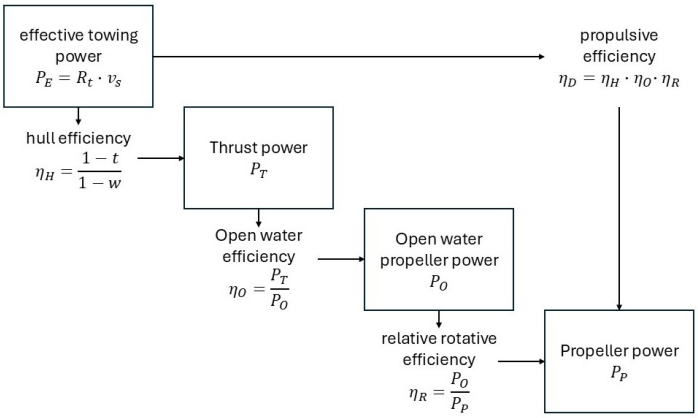

Figure 5.5: The efficiencies relating P_E to P_P, with intermediate powers (Klein Woud & Stapersma, 2002)

First, the effective towing power P_E is calculated by multiplying R_t with v_s. Next, the hull efficiency η_H describes the ratio of thrust deduction $(1-t)$ to wake fraction $(1-w)$. Thrust deduction is a result of the suction effect at the stern induced by the rotating propeller. The wake fraction accounts for the difference in axial inflow speed that a propeller rotating behind a hull was to experience if it was operating in open water (Vervoordeldonk, 2025). For a (semi-)planing hull, it is hard to predict the thrust deduction factor and the wake fraction, since the shape of the displacement volume and the hydrodynamic interactions between the hull and the water depend on the vessel speed. For now, η_H is estimated to be 0.9 on average.

Then, the open water efficiency η_O of a propeller describes how well the propeller can convert its

rotational kinetic energy into effective thrust power. Similar to η_H, the open water efficiency of the of the propeller also depends on the propeller design, the vessel speed and the generated thrust force. With the predicted P_E the open water efficiency of a B4-70 Wageningen propeller (a typical propeller for a patrol vessel) is calculated using PropCalc. This gives an average open water propeller efficiency of roughly 0.65.

Finally, the relative rotative efficiency η_R accounts for the mixed wake and open water flows in the wake field, and usually lies between 0.95 and 1.05 (Carlton, 2007). As to be conservative, it is taken as 0.97 for now.

More extensive research is needed to validate the values of each individual value of η_H, η_O and η_R. However, when the combined efficiency η_D is used to calculate the required shaft power, the results can be compared to the shaft power measurements of an actual full scale RWS vessel. JVS has measured the shaft power of the RWS 22 and the RWS 82. Both vessels have a length of 18.8 m, a width of 5.25 m, and a maximum draught of 1.25 m, and both have a combined installed power of 810 kW. The comparison of shaft power is shown in figure 5.6.

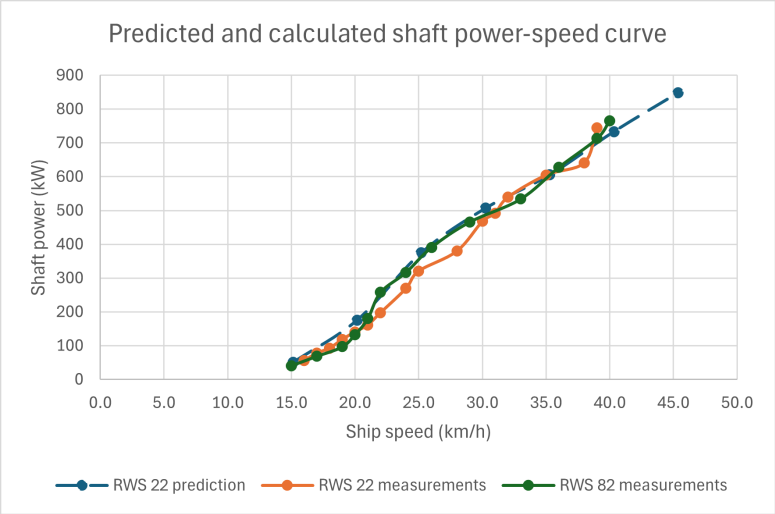

Figure 5.6: The predicted and measured shaft power of the RWS 22 and the RWS 82

The predicted and measured values show a high level of congruency with one another. Note that the density of predicted data points below 20 km/h is lower than that of the measured values, and the accuracy of the predictions between 15 and 20 km/h is therefore harder to test. However, in the most extreme shifts, most energy is spent at intermediate and full speed. Therefore, the accuracy of the results of this research depend more heavily on the shaft power predictions at high speeds, rather than the low speeds.

Further, the predicted shaft power at full speed of both vessels is close to 760 kW, which is 50 kW (or 6%) short of the total installed power of 810 kW. This power is attributed to the on-board auxiliary systems like pumps and lights. In the iteration process in paragraph 6.1, the required total installed power is assumed to be 106% of the maximum required shaft power.

6

Zero-emission power plant feasibility

With a method to predict m_{pp} as a function of P_E established in chapter 4, and a method to predict P_E as a function of m_{pp} established in chapter 5, the feasibility of each energy carrier can now be tested through the process of iteration. Paragraph 6.1 gives an overview of the iterating process and the results of the feasibility study. In paragraph 6.2 a layout is suggested for the most preferred feasible design in each region type.

6.1. Promising configurations

An overview is made of the initial values of m_{PP} for every configuration in all three regions, shown in table 6.1.

Table 6.1: Initial calculated m_{PP} for the reference vessels for each configuration

	Battery-electric	Battery-Fuel cell hybrid ($r_{batt} = 10\%$)	H2 ICE	Methanol ICE	Battery-methanol hybrid ($r_{batt} = 10\%$)
Region I	31.0 t	22.8 t	23.5 t	14.6 t	18.7 t
Region II	50.5 t	35.4 t	35.9 t	21.0 t	26.9 t
Region III	13.1 t	10.9 t	11.8 t	8.5 t	11.0 t

In the hybrid configurations r_{batt} is set to 10%, since this gives the lowest total weight for the hybrids. If it can be shown that the hybrid is not feasible at the lowest possible weight of that configuration, then by extension that specific hybrid is not feasible for every other value of r_{batt}. If the hybrid is feasible at 10% and there is no other feasible configuration that is preferred by RWS, then that configuration is to be investigated to find the maximum possible r_{batt}.

First, the feasibility of each configuration is checked for type I regions. The RWS 21 is used as a reference for the estimation of the resistance and the power plant weight of a diesel powered type I region vessel. It has a displacement of roughly 32 m^3, an installed power of 909 kW, and it can reach speeds of up to 22 kn. The total diesel power plant weight is estimated to be 8.4 t, which is estimated following the same method used by MARIN to estimate the power plant weight of a patrol vessel with an installed power of 1360 kW, as described in paragraph 4.1.

The battery-methanol ICE hybrid power plant weight is estimated to be 18.7 t. This means the total vessel weight with the new power plant would be 32 t + (18.7 t - 8.4 t) = 42.7 t. The draught, beam and length of the 3D model is adjusted to meet the new displacement requirement. Next, the DSDS calculation is done again to find the vessel's new resistance and required P_E. With this P_E the new power plant size is calculated. This time, it is estimated at 49.1 t. Continuing this process in this case leads to such a severe increase in the vessel's draught and main dimensions that the vessel becomes

too large for the activities of RWS in type I regions. Therefore, the battery-methanol hybrid is deemed not feasible for type I regions, and configurations with a heavier initial m_{PP} will a fortiori also not be feasible.

This leaves the methanol ICE configuration. When the same process is repeated for the methanol ICE configuration, the vessel weight and power plant weight converge with ship dimensions that support operation in type I regions. The main vessel specifications are shown in table 6.2.

Table 6.2: The estimated specifications of a vessel powered by a methanol ICE in a type I region

	RWS 21	**Methanol ICE design**
L_{oa}	18.8 m	19.7 m
B_{oa}	5.25 m	5.35 m
T	1.05 m	1.19 m
Δ	32.0 t	45.8 t
P_{ins}	909 kW	1397 kW

As shown, the new vessel can have an increased length and width compared to the reference vessel. When increasing the main dimensions of the vessel, an increase in the structural weight of the ship must be taken into account, since extra steel is needed for lengthening and broadening. For an increase in length, a rough estimation of the total area of steel in a midsection of the ship is made. It is assumed that a midsection consists of the main deck, the inner and outer bottom, and the inner and outer sides. Likewise, broadening the vessel also imposes an increase in structural weight. In that case, the stern and bow, main deck, and inner and outer bottom, as well as 4 bulkhead are taken into account for the cross-sectional steel area of a buttock. Further, a steel thickness 8 mm is assumed and 20% steel volume is added to account for the stiffening. Given that the vessel is made out of S235 steel with a density of 7850 kg/m^3 (Eurocode Applied, n.d.), the total added structural weight is calculated as a function of added length compared to the RWS 21.

For type II regions, the RWS 71 is used as a reference. The weight of the power plant is estimated at 12.8 t as per the MARIN calculations in paragraph 4.1, and the general arrangement plans report a designed vessel displacement of 57 m^3. Following the same protocol as was described previously for a region I vessel, it is found that the methanol ICE configuration is the only feasible configuration in regions of type II. However, without any operational adjustments, the required size increase is expected to limit the vessel's operation to a too large extent, for example in small harbours or locks. To mitigate this, the maximum speed can be reduced to 40 km/h, or the bunker frequency can be increased. Table 6.3 shows the results of the convergence study for either of these scenarios, and these scenarios combined.

Table 6.3: The estimated specifications of a vessel powered by a methanol ICE in a type II region

	RWS 71	Methanol ICE design (No operational adjustments)	Methanol ICE design (Max speed red. to 40 km/h)	Methanol ICE design (Bunker frequency incr. to 1.5 days)	Methanol ICE design (Incr. bunker frequency & red. max speed)
L_{oa}	23.95 m	26.7 m	25.9 m	25.3 m	25.0 m
B_{oa}	5.59 m	6.13 m	6.14 m	5.72 m	5.65 m
T	1.32 m	1.40 m	1.40 m	1.40 m	1.37 m
Δ	57.0 t	80.0 t	75.7 t	68.9 t	65.4 t
P_{ins}	1302 kW	1988 kW	1624 kW	1691 kW	1327 kW

Apart from operational adjustments, decreasing the total vessel weight is another way to enable operation on methanol. For example, the hull of the RWS 70-series vessels is made out of steel. Using aluminium, with a density close to a third of that of steel, would decrease the total vessel weight by a large margin. Next to this, some equipment in the current vessels might not be used, and can therefore be stripped from the vessel. An example of this, according to crew members, is too much benches and tables below deck left unused by the crew, or the octopus body recovery unit. A crew member stated never to have used the Octopus in over 50 body recoveries, since it is only usable in very specific cases. Inquiry with crew members into what systems are left unused might result in options for significant weight reduction, increasing the applicability of alternative fuels.

Figure 6.1 shows how much weight reduction compared to the RWS 70-series is required to operate in a type III region with a methanol ICE. With increasing total displacement weight, the length gradually increases from 23.95 m to 26.7 m, the beam from 5.59 m to 6.13 m and the draught from 1.32 m to 1.40 m. For instance, an RWS 70-series vessel is used as reference vessel, with a maximum speed of 45 km/h and a minimum time between bunkers of 2 days. Its dimensions are scaled so it has an increased displacement of 70 t to account for the heavier methanol components compared to diesel. In that case, the graph shows that 4 t must still be stripped from the vessel to allow for implementation of methanol. Or in reverse: if stripping unnecessary equipment and switching from steel to aluminium saves a total of 8 t on the RWS 70-series, and that vessel was to operate on a methanol ICE, then the total vessel weight would converge to roughly 62.5 t.

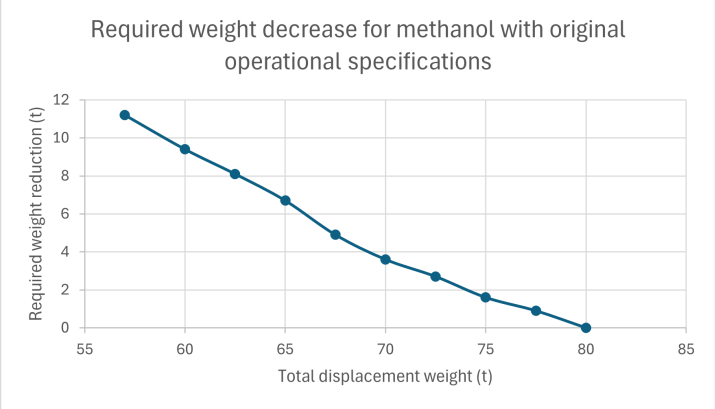

Figure 6.1: The required weight loss compared to the RWS 70-series vessels to operate on methanol in a type III region

The region III convergence study shows that a battery-electric configuration is feasible. The increase in displacement can only be achieved by increasing the vessel length and beam, since the draught of the RWS 59 is already equal to the maximum allowed draught. The main parameters of a battery-electric powered vessel in a type III region are shown in table 6.4.

Table 6.4: The estimated specifications of a battery-electric vessel in a type III region

	RWS 59	Battery-electric region III vessel
L_{oa}	19.45 m	20.17 m
B_{oa}	5.2 m	5.43 m
T	1.4 m	1.4 m
Δ	82.6 t	91.4 t
P_{ins}	588 kW	719 kW

The total resistance-speed curve of the type III region vessel, found using the method by Holtrop & Mennen, is shown in figure 6.2.

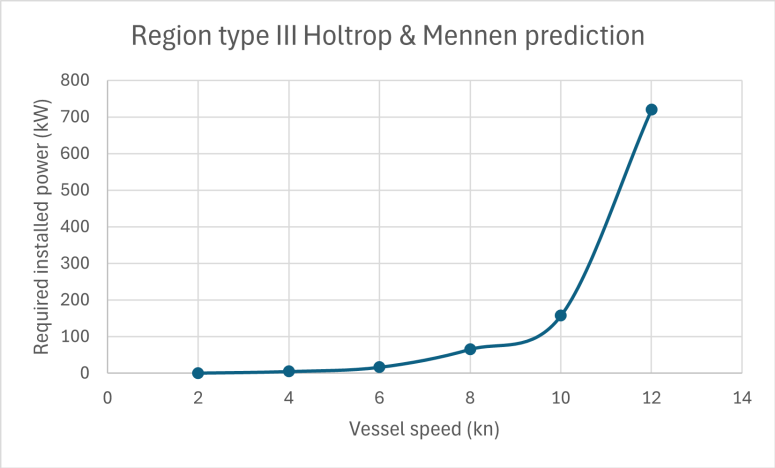

Figure 6.2: The required installed power of a vessel in region type III as a function of vessel speed, predicted using the method by Holtrop & Mennen

Since the battery-electric configuration, which is RWS' first preference, is found to be feasible, the other configurations are not further investigated. By extension, the battery-fuel cell hybrid and the methanol ICE configurations are also feasible when only taking into account weight and resistance, since their initial estimated weight is lower than that of the battery-electric configuration, as table 6.1 shows. Whether these configurations require adjustments to the original RWS 59 is not looked into. The feasibility of the H_2 ICE configuration and the battery-methanol hybrid require further research in order to draw conclusions on their feasibility. The results of the feasibility study are summarised in table 6.5. Note that these results are based on convergence between m_{PP}, P_E and R_t.

Table 6.5: Results of feasibility study based on weight and resistance.

	Battery-electric	Battery-fuel cell hybrid	H2 ICE	Methanol ICE	Battery-methanol hybrid
Region I	Not feasible	Not feasible	Not feasible	Feasible on RWS 21 with adjustments	Not feasible
Region II	Not feasible	Not feasible	Not feasible	Feasible on RWS 71 with adjustments	Not feasible
Region III	Feasible on RWS 59 with adjustments	Feasible on RWS 59 (with adjustments)	Feasible on RWS 59 (with adjustments)	Feasible on RWS 59 (with adjustments)	Further research needed

For region types I and II, only methanol, the carrier least preferred by RWS, is deemed feasible. Decreasing the maximum speed and decreasing the minimum time between bunkers are measures to decrease the total required stored energy, as shown in table 6.3. However,

6.2. Suggestions for a general layouts

For each region type, the most promising energy configuration has been identified. Next, an example layout is presented for each design.

6.2.1. Layout type I region

The methanol ICE configuration is the only feasible configuration in regions of type I. A suggested general layout of the design is shown in figure 6.3.

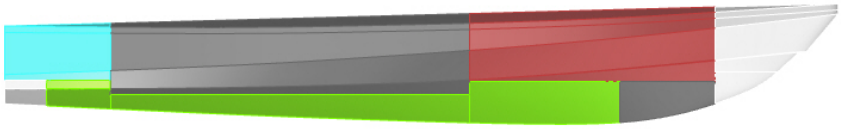

Figure 6.3: A suggestion of a general layout for a methanol powered vessel in a type I region. (Green; methanol storage, grey; machinery space, brown; accommodation, blue; cooling systems, white; collision spaces and water tanks)

The bulkhead and deck locations are similar to that of the RWS 21. However, the bulkhead forward of the engine room is moved forward, effectively sacrificing some accommodation space to gain space for machinery in the engine room. This is done, because, based on crew statements, not all accommodation space is strictly needed, and the machinery space is expected to be somewhat larger than a machinery space equipped for diesel power.

An advantage of storing methanol, compared to storing diesel, is that it can be stored directly against the outer hull, if a tank is located below the lowest possible waterline, as prescribed by Bureau Veritas in section 3, paragraph 1.2.2 of rules regarding methanol fuelled ships (Bureau Veritas, 2024). A downside is that in the case of a type I region, the required storage volume is more than four times larger than the diesel powered RWS 21. The storage volume reserved for methanol in the double bottom, depicted in green, equals a total of roughly 15 m^3, and is located entirely under the waterline. The cumulative surface area of the required aft, forward and top steel cofferdams is approximately 50 m^2.

Alternative to storing the methanol in the double bottom, a more compact tank design may be considered. In figure 6.4, an example of such a methanol tank design is shown. Assuming one of the two transverse cofferdams is created by locating the tank such that the aft or forward surface of this tank coincides with a transverse bulkhead, the total surface area of the tank is approximately 46 m^2. In this case, storing methanol in a more compact tank that stretches above the waterline saves less than 10% of surface material needed for the tanks. Considering this storage location occupies space that can be used for machinery or accommodation, while leaving the double bottom essentially unused, storage in the double bottom is preferred.

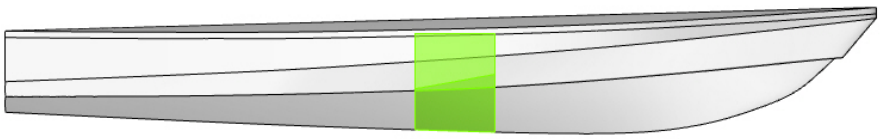

Figure 6.4: An example of methanol storage in a tank more compact than storage in the double bottom

6.2.2. Layout type II region

For region II type vessels, methanol is also the only feasible energy configuration. Figure 6.5 shows a suggested layout of such a vessel.

Figure 6.5: A suggestion of a general layout for a methanol powered vessel in a type II region. (Green; methanol storage, grey; machinery space, brown; accommodation, blue; cooling systems, white; collision spaces and water tanks)

Similar to the region I vessel, the methanol storage is again placed in the bottom of the hull. The storage shown in the figure can hold a total of 21.0 m^3, and is located entirely under the waterline. Further, part of the accommodation space is again sacrificed to make room for the machinery space, that will be larger due to the increase in required power compared to the RWS 70 series vessels.

A more compact methanol tank design is analysed to determine how much tank steel can be saved, similar to the analysis executed on the type I region vessel. The tank shown in figure 6.5 has a total cofferdam area of approximately 63 m^2. A more compact tank that uses a transverse bulkhead as one of its cofferdams would need approximately 57 m^2 of cofferdam area. This would save close to 12% of steel material on the storage tanks, while leaving the double bottom unused and occupying space that could otherwise be used as machinery or accommodation space. Therefore, storage in the double bottom is preferred to storage in a central compact tank.

6.2.3. Layout type III region

The type III region vessel is powered by batteries. A suggestion of a general layout of the vessel is provided in figure 6.6.

Figure 6.6: A suggestion of a general layout for a battery powered vessel in a type III region. (Yellow; batteries, grey; generator room, brown; accommodation, blue; cooling systems, white; collision spaces and water tanks)

The locations of the bulkheads and decks in the suggested design are based on the general arrangement of the RWS 59. The main difference is that the engine room is split into two parts, one battery storage space and one generator room. This is necessary, since Bureau Veritas imposes that Li-ion batteries exceeding a capacity of 20 kWh 'are to be installed in a dedicated space that is not located forward of the collision bulkhead' in sec 11, art. 6.5 in their rules for steel ships (Bureau Veritas, 2025a). This means that the batteries may also be stored in the space most aft in the vessel, although this may adversely affect the vessel's trim and transverse stability. The battery space that is shown can hold around 96 batteries, while the predicted required amount is 88. If necessary, the accommodation space can be moved further forward or made smaller to dedicate more space to the generator room.

7

Conclusion

7.1. Conclusion

This thesis is aimed to answer the research question:

How can the Rijksrederij patrol vessel fleet be turned climate neutral and preferably emission free within the operational demands, by adopting batteries, hydrogen or methanol as an energy carrier?

In support of this research question, three sub-questions are defined. The first question is posed to define the operational framework of the Rijksrederij fleet:

What are the patrol vessel's relevant operational requirements and what are the characteristics of the different patrol areas?

The Rijksrederij manages patrol vessels in a variety of areas in the Netherlands. Each area has its own corresponding operational requirements for the vessel. These requirements are mainly based on the wave sensitiveness of the area and how far the area is stretched out. All areas can roughly be categorised in 3 distinct region types:

Regions of type I are mainly large rivers, that are only partly wave sensitive, but cover a moderate amount of distance. A maximum vessel dimensions are imposed by crew preference to ensure that their operations can still be carried out.

Regions of type II are not wave sensitive, and are stretched out further than type I regions. This includes for example large lakes. These regions require a large energy capacity compared to the other two types, because of the high speeds and long travel distances. A large vessel is called for to mitigate the effects of heavy weather on the vessel on open water.

Regions of type III cover all wave sensitive areas, and are relatively small, like canals or small lakes. Therefore, the vessels that operate in these regions do not require a high top speed and a large range. Thus, the energy capacity for vessels in this region type is lower than the other two region types.

The second research focusses on the differences between vessels powered by diesel and alternative fuels:

How does the adoption of the energy carriers influence the design requirements relative to a fossil powered vessel?

This question is answered by estimating the total power plant weight and size, if they were equipped on 3 vessels that each typically operate in one of the three operating regions. Of the three energy carriers mentioned in the main research question, batteries require the heaviest power plant and hydrogen requires the largest power plant, while methanol is the lightest and most compact. However, methanol is not necessarily the best option for the operation of the Rijksrederij, since batteries and hydrogen are preferred over methanol because of its emissions.

Therefore, the third research question is defined:

Which energy carriers are best suited for the Rijksrederij's patrol vessels?

This question is answered by evaluating the increase in resistance and required power of the typical vessels in each region when equipped with alternative fuels. By iterating between the power plant weight and the increased resistance, methanol was identified as the only feasible option for operation in type I and type II regions. In type III regions, batteries are a feasible option as an energy carrier. After evaluation of the spacial arrangement in the vessels, the main research question can be answered:

The Rijksrederij patrol fleet can be turned climate neutral, but not emission free, by adopting batteries and methanol as energy carrier. Batteries are to be used in relatively small operating regions with strict speed limitations, while methanol is to be used on vessels operating in larger regions that allow for operation at higher speeds.

7.2. Discussion

The credibility of the results of this thesis is subject to several factors that are hard to predict or determine, without further research.

First, the intended goal of the the adoption of alternative energy carriers is to realise a climate neutral operation. However, the operation can only be considered climate neutral if the fuels are produced through a renewable process. This is a prerequisite for the RWS operation to become climate neutral through adoption of alternative fuels.

Next, the defined operational framework is based on observations of four shifts in two different region types, statements from crew members and an operational supervisor, and an AIS-data analysis. Each of these sources inherently possess a degree of unreliability. Observations on four shifts (none of which were to be considered somewhat extreme) provide an overview of the main activities of the RWS during an average day, but do not give clear insight into an extreme operating day; crew statements may be under- or overstated, and for a large part anecdotal; the AIS-data analysis is based on data of six different vessels, providing only a general overview of the operations in six different areas, and a portion of the data points are filtered out before the analysis because of GPS faults. The reliability of the total required energy storage is therefore limited.

Third, the size and weight of the power plant are predicted by evaluating each individual component in the power plant. However, the specifications of some can be more reliably predicted than of others. The weight of batteries can be calculated with a high level of accuracy, since these are a readily available product with a given weight and size. In contrast, the weight needed for the transportation of hydrogen on board is more complex, since this involves an infrastructure with several pipes and valves. Likewise, the prediction of the insulation weight is hardly a precise number, since the layout of the vessel is key to the amount of insulation needed, and this layout is prone to the preference of Rijkswaterstaat. Subsequently, a more precise evaluation of the components in the power plants will provide a more robust conclusion regarding the feasibility of all configurations in each region.

Additionally, the scale of alternative fuel use is still small and the technologies underdeveloped, compared to diesel. This can affect positively and negatively affect the feasibility of alternative energy carrier implementation.

The feasibility of each fuel depends on the availability, price and transport infrastructure of each fuel. Infrastructure has yet to be installed. In the meantime, vessels rely on fuel supply by trucks. If the needed amount of fuel exceeds the amount the trucks can deliver, the RWS operation is essentially limited. Also, if hydrogen is transferred from the truck to the tanks using the pressure difference as a driving force, then equilibrium pressure might be lower than 350 bar, causing the total hydrogen storage to be lower than the designed storage capacity. These factors may negatively influence the feasibility of each carrier.

On the other hand, since the alternative energy carrier technology is relatively young, current research into alternative energy carriers is driving technological developments, leading to increased power and energy storage densities, and higher energy efficiencies. Hence, the feasibility of each energy carrier might increase in the future.

Then, the input values for the resistance prediction are measured using the 3D models. These models are only a rough approximation of the actual operating vessels. This decreases the reliability of the esti-

mations. Also, the resistance prediction methods themselves, combined with the estimated propulsive efficiency provide a rough estimate of the required installed power of the vessels. CFD simulations or scale model tests can provide more accurate insight in the actual required installed power.

Finally, the stability of the vessels is not checked. This requires a more detailed layout design, to know where each weight component is installed. Stability could potentially be a limiting factor on all vessels. Methanol storage in the double bottom may act as a mitigating factor for the heavier methanol systems (compared to diesel systems) located higher up in the ship. For region type III, heavy battery walls are likely to be installed, stacked to a certain height. Whether this will pose a stability problem, and thus affect the feasibility of batteries as an alternative energy carrier, was not analysed in this thesis.

7.3. Recommendations

In addition to the findings in this thesis, it is recommended to look into several related research topics:

First of all, the RWS may be able to save energy by reorganising its operation. Moored vessels and on-shore locations like docks can be travelled to by car, instead of boat. And on days with little to no expected traffic and no planned inspections, patrol routes can be shortened or maybe even skipped. Further, if an inspection is planned at a great distance from the RWS berth location, it might be beneficial to have a smaller, more energy efficient vessel, rather than a large, heavy vessel for long trips to save energy.

Second, an inquiry into the necessity of current on-board equipment is recommended to ensure the vessels in the new fleet are kept as light as possible. This way, a larger part of the load capacity can be reserved for heavy alternative fuel power plants, and less energy is needed for the operation, which in turn also decreases the weight of the on-board storage facility. Interviews with crew members can provide useful information regarding the usefulness of equipment.

Next, more on-shore locations with fast recharging facilities can decrease the total required energy storage capacity on board. If full packs of batteries are readily available and rapidly exchangeable at multiple sites on routes that are known to be travelled often by patrol vessels, then less storage capacity is needed on board. This would decrease the power plant weight of battery powered vessels, and increase its feasibility.

This thesis uses the current vessel fleet as a reference. Other hull structures are not analysed. Multi-hulls or hydrofoils might present significantly lower energy demands at higher speeds, at which most energy is consumed. A hull vane could also save energy. If optimised for high speed operation, its savings at high power demands could outweigh the increased resistance of the vane at lower speeds, for which it is not designed. Further, the use of hybrid systems may decrease the total emissions of a vessel. In this thesis, the hybrid configurations are designed for several subsequent extreme shifts, assuming all energy that is bunkered is also used. However, in a large share of all shifts, the vessel sail mostly slow. A battery-methanol ICE hybrid might therefore not need to sail on methanol for days on end, essentially turning an electric-fossil hybrid into an entirely emission-free vessel, as a result of always using the electrical energy first. It is recommended to perform an analysis on what the actual electrical to fossil energy consumption ratio is.

Finally, alternative energy carrier technologies are extensively researched worldwide. The energy efficiency, power and energy density, and safety measures improve with the development of new technologies. Therefore, it is recommended to re-evaluate the feasibility of batteries, hydrogen and methanol against the yardstick of the latest technological developments. In the same line of thought, others carriers than the three considered in this thesis might become serious contenders for climate neutral operation in the future.

References

AlZohbi, G., Almoaikel, A., & AlShuhail, L. (2023). An overview on the technologies used to store hydrogen. *Energy Reports*, *9(11)*, 28–34. https://doi.org/10.1016/j.egyr.2023.08.072

Artemis Technologies. (n.d.). *New Fully Electric Patrol Vessel Springs Into Action at the Port of Rotterdam* [Retrieved August 14, 2025]. https://www.autoevolution.com/news/new-fully-electric-patrol-vessel-springs-into-action-at-the-port-of-rotterdam-252194.html#agal_1

AYK. (n.d.). *The provider of key energy storage system* [Retrieved March 14, 2025]. https://www.aykenergy.com/products

Ballard. (2024). *Fuel Cell Power Module for Marine Applications* [Retrieved April 8, 2025]. https://www.ballard.com/wp-content/uploads/2024/11/FCwave_20241008.pdf

Battery University. (2021). *BU-808c: Coulombic and Energy Efficiency with the Battery* [Retrieved March 26, 2025]. https://batteryuniversity.com/article/bu-808c-coulombic-and-energy-efficiency-with-the-battery

Beyond Motors. (n.d.). *AXM4*. https://cdn.prod.website-files.com/6374bfb931e7186e3b5586b6/67417bcbaca8a1100c90ae5a_AXM4.pdf

Buckley, J. (2023). *Cummins holds China unveil of X15H hydrogen IC* [Retrieved July 20, 2025]. https://www.powerprogress.com/news/cummins-holds-china-unveil-of-x15h-hydrogen-ic-engine/8031246.article

Bureau Veritas. (2024). *Methanol and ethanol-fueled ships* (tech. rep. No. NR670). https://erules.veristar.com/dy/data/bv/pdf/670-NR_2024-07.pdf

Bureau Veritas. (2025a). *Article 6 Storage batteries* [Retrieved July 27, 2025]. https://erules-svc.veristar.com/dy/app/ui-bv-steelships-steelships_2025-search-batteries.do#n00010003000200110006

Bureau Veritas. (2025b). *Rules for the classification of steel ships* (tech. rep. No. NR467). https://erules.veristar.com/dy/data/bv/pdf/467-NR_PartB_2025-01.pdf

Carlton, J. (2007). Marine propellers and propulsion. Elsevier Ltd.

co2emissiefactoren.nl. (2024). *Lijst emissiefactoren* [Retrieved on August 2, 2024]. https://www.co2emissiefactoren.nl/lijst-emissiefactoren/

Corvus Energy. (n.d.-a). *Corvus Dolphin NxtGen ESS – Energy* [Retrieved March 14, 2025]. https://corvusenergy.com/products/corvus-dolphin-nxtgen-ess-energy#specs

Corvus Energy. (n.d.-b). *Pelican Marine Fuel Cell System* [Retrieved April 8, 2025]. https://corvusenergy.com/products/corvus-pelican-marine-fuel-cell-system

Danfoss. (n.d.). *Electric motors*. https://www.danfoss.com/en/products/dps/electric-converters-motors-and-systems/electric-motors-and-generators/electric-motors/#tab-overview

Demaco. (n.d.). The energy density of hydrogen: A unique property [Retrieved September 10, 2024]. https://demaco-cryogenics.com/blog/energy-density-of-hydrogen/

Dere, C. (2023). Hydrogen Fueled Engine Technology, Adaptation, and Application for Marine Engines. In B. Zincir, P. C. Shukla, & A. K. Agarwal (Eds.), *Decarbonization of Maritime Transport* (pp. 45–63). Springer Nature Singapore. https://doi.org/10.1007/978-981-99-1677-1_4

DNV. (2021). Handbook for hydrogen fueled vessels. https://www.iims.org.uk/wp-content/uploads/2021/07/Handbook_for_hydrogen-fuelled_vessels.pdf

Elzenga, H., & Strengers, B. (2024). *Productie, import, transport en opslag van waterstof in nederland* (PBL Rep. No. 5206). Planbureau voor de leefomgeving. https://www.pbl.nl/system/files/document/2024-04/pbl-2024-productie-import-transport-en-opslag-van-waterstof-in-nederland_5206.pdf

Emrax. (n.d.). *Emrax 348*. https://emrax.com/e-motors/emrax-348/

EST-floattech. (n.d.). *Octopus Series* [Retrieved March 14, 2025]. https://www.est-floattech.com/wp-content/uploads/2024/08/Specsheet-Octopus-Series.pdf

Eurocode Applied. (n.d.). *Table of design material properties for structural steel* [Retrieved July 26, 2025]. https://eurocodeapplied.com/design/en1993/steel-design-properties

Evolito. (n.d.). *Axial Flux Electric Motors: A Revolutionary Approach*. https://evolito.aero/axial-flux-motors/#D1700:%20High%20torque,%20low%20speed.

flashbattery.tech. (n.d.). *Which chemistry is most suitable for the electrification of your vehicle? Let's discover the different types of batteries*. https://www.flashbattery.tech/en/types-of-lithium-batteries-which-chemistry-use/

GESAMP. (2019). *Gesamp hazard evaluation procedure for chemicals carried by ships, 2019* (Rep. Stud. GESAMP No. 102). GESAMP. International Maritime Organization. http://www.gesamp.org/site/assets/files/2133/rs102e.pdf

Heidinga, K. (2020). 12 juni 2020 t.h.v. wijhe. https://varenderfgoed.nl/dv/rws59.html

Heidinga, K. (2021). 22 april 2021 op urk. https://varenderfgoed.nl/dv/rws77.html

Hemken, D. (2025). 11 april dordtse kil. https://varenderfgoed.nl/dv/rws21.html

Hexagon Purus. (2025). *Hydrogen high-pressure Type 4 cylinders* [Retrieved July 17, 2025]. https://d2unncwr0d5wwb.cloudfront.net/purus/HPU_0225_02_Datenblatt_Type4_Mobility.pdf

Holtrop, J., & Mennen, G. (1982). An approximate power prediction method. *International Shipbuilding Progress*, *29, 335*. https://doi.org/10.3233/ISP-1982-2933501

Horizon Educational. (n.d.). *150kW Liquid cooled Fuel Cell VL-Series* [Retrieved April 12, 2025]. https://www.horizoneducational.com/150kw-liquid-cooled-fuel-cell-vl-series/p1574

Hydrogenics. (n.d.). *HyPM HD 180* [Retrieved April 8, 2025]. https://pdf.directindustry.com/pdf/hydrogen-systems/hypm-hd180/14703-316895.html

Hydrosta. (n.d.). *Parallel Hybrid Propulsion HP Inline* [Retrieved July 19, 2025]. https://hydrosta.nl/uploads/documents/FolderHPInLine.pdf

IenW. (2023a). *Hoe is dit verslag tot stand gekomen?* [Retrieved August 2, 2024]. https://magazines.rijksoverheid.nl/ienw/duurzaamheidsverslag/2023/01/over-dit-duurzaamheidsverslag

IenW. (2023b). *Strategie Klimaatneutrale en Circulaire Organisatie* [Retrieved August 1, 2024]. https://magazines.rijksoverheid.nl/ienw/duurzaamheidsverslag/2023/01/strategie-klimaatneutrale-en-circulaire-organisatie

IenW. (n.d.). *Energie en klimaat* [Retrieved August 1, 2024]. https://www.rijkswaterstaat.nl/leefomgeving/energie-en-klimaat

Incat Crowther 19. (n.d.). *Incat Crowther 19* [Retrieved August 14, 2025]. https://www.incatcrowther.com/ships/defence/patrol-boats/ic16108/

IPCC. (2018). Annex i: Glossary. In V. Masson-Delmotte, P. Zhai, H.-O. Pörtner, D. Roberts, J. Skea, P. R. Shukla, A. Pirani, W. Moufouma-Okia, C. Péan, R. Pidcock, S. Connors, J. B. R. Matthews, Y. Chen, X. Zhou, M. I. Gomis, E. Lonnoy, T. Maycock, M. Tignor, & T. Waterfield (Eds.), *Global warming of 1.5°c: Ipcc special report on impacts of global warming of 1.5°c above pre-industrial levels in context of strengthening response to climate change, sustainable development, and efforts to eradicate poverty* (pp. 541–562). Cambridge University Press, Cambridge, UK and New York, NY, USA. https://doi.org/10.1017/9781009157940.008

IRENA. (2021). A pathway to decarbonise the shipping sector by 2050. International Renewable Energy Agency Abu Dhabi.

Isover Saint-Gobain. (n.d.-a). *Aluminium Bulkhead A60 Full Comfort* [Retrieved July 20, 2025]. https://www.isover-technical-insulation.com/node/6346

Isover Saint-Gobain. (n.d.-b). *Aluminium Deck A60 4 mm Full Comfort* [Retrieved July 20, 2025]. https://www.isover-technical-insulation.com/node/6336

Janek, J., & Zeier, W. (2023). Challenges in speeding up solid-state battery development. *Nat Energy*, *8, 230-240*. https://doi.org/10.1038/s41560-023-01208-9

Jung, W., Choi, M., Jeong, J., Lee, J., & Chang, D. (2024). Design and analysis of liquid hydrogen-fueled hybrid ship propulsion system with dynamic simulation. *International Journal of Hydrogen Energy*, *50*, 951–967. https://doi.org/https://doi.org/10.1016/j.ijhydene.2023.09.205

Kachi, A., Mooldijk, S., & Warnecke, C. (2020). *Climate Neutrality Claims*. https://newclimate.org/sites/default/files/2020/09/Climate_neutrality_claims_BUND_September2020.pdf

Kartini, E., & Genardy, C. (2020). The future of all solid state battery. *IOP Conf. Ser.: Mater. Sci. Eng.*, *924*, 012038. https://doi.org/10.1088/1757-899X/924/1/012038

Keuning, L., & Hillege, W. (2017). The results of the delft systematic deadrise series. In *Proceedings of 14th international conference on fast sea transportation (fast 2017): Innovative materials* (pp. 97–106). FAST Organizing Committee.

Klein Woud, H., & Stapersma, D. (2002). Design of propulsion and electric power generation systems. Institute of Marine Engineering, Science; Technology.

Li, J.-C., Xu, H., Zhou, K., & Li, J.-Q. (2024). A review on the research progress and application of compressed hydrogen in the marine hydrogen fuel cell power system. *Heliyon*, *10(3)*, e25304. https://doi.org/10.1016/j.heliyon.2024.e25304

Lubex. (2023). *LUBEX MITRAS ATF II* [Retrieved July 19, 2025]. https://lubex.com.tr/media/1709/lubex-mitras-atf-ii.pdf

MAN Engines. (2023). *MAN Engines presents groundbreaking hydrogen combustion engine for off-road applications* [Retrieved July 16, 2025]. https://press.mantruckandbus.com/corporate/man-engines-presents-groundbreaking-hydrogen-combustion-engine-for-off-road-applications/

MAN Engines. (n.d.). *Hydrogen engine: a climate-friendly alternative* [Retrieved August 14, 2025]. https://www.man.eu/engines/en/in-focus/engines/hydrogen-engine-a-climate-friendly-alternative-127808.html

MAN Rollo. (n.d.). *Marine high speed propulsion engines* [Retrieved July 17, 2025]. https://manrollo.com/wp-content/uploads/Marine_Commercial_220512_web-website.pdf

Manualslib. (n.d.). *Dimensions; Unpacking The Equipment - Parker MAXIGAS MX104 User Manual* [Retrieved July 19, 2025]. https://www.manualslib.com/manual/1588637/Parker-Maxigas-Mx104.html?page=7#manual

MARIN. (2020). *Sustainable Power* [Retrieved April 12, 2025]. https://sustainablepower.application.marin.nl/table

Marine Service Noord. (n.d.). *Methanol fuel tanks* [Retrieved August 14, 2025]. https://marine-service-noord.com/en/products/alternative-fuels-and-technologies/methanol/methanol-fuel-tanks/#:~:text=Tanks%20containing%20fuel%20should%20not,Portable%20tanks

Melançon, S. (2023). *Comparing six types of lithium-ion battery and their potential for BESS applications*. https://www.energy-storage.news/comparing-six-types-of-lithium-ion-battery-and-their-potential-for-bess-applications/

Methanol Institute. (2022). *Carbon footprint of methanol* (tech. rep.). https://www.methanol.org/wp-content/uploads/2022/01/CARBON-FOOTPRINT-OF-METHANOL-PAPER_1-31-22.pdf

Methanol Institute. (n.d.-a). *Physical Properties of Pure Methanol* [Retrieved July 16, 2025]. https://www.methanol.org/wp-content/uploads/2016/06/Physical-Properties-of-Pure-Methanol.pdf

Methanol Institute. (n.d.-b). *The Methanol Industry* [Retrieved September 18, 2024]. https://www.methanol.org/the-methanol-industry/

MG. (2025). *Product data sheet* [Retrieved August 12, 2025]. https://downloads.mgenergysystems.eu/api/v1/resources/3e994ae9-a561-4a4c-a92a-17a6f0eb2589?inline=true

Miao, Y., Hynan, P., von Jouanne, A., & Yokochi, A. (2019). Current li-ion battery technologies in electric vehicles and opportunities for advancements. *Energies*, *12(6)*, 1074. https://doi.org/10.3390/en12061074

Park, S.-J., Song, Y.-W., Kang, B.-S., Kim, W.-J., Choi, Y.-J., Kim, C., & Hong, Y.-S. (2023). Depth of discharge characteristics and control strategy to optimize electric vehicle battery life. *Journal of Energy Storage*, *59*, 106477. https://doi.org/https://doi.org/10.1016/j.est.2022.106477

Phi-power. (n.d.). *Ph-Range* [Retrieved July 19, 2025]. https://www.phi-power.com/en/phi-power-motor-series-2/racing-high-performance/

Phi-power AG. (n.d.). *PH38X series*. https://www.phi-power.com/wp-content/uploads/2018/05/PH382-Spec_Sheet-V1.3.pdf

PowerCell. (n.d.). *Marine System 225* [Retrieved April 11, 2025]. https://25513287.fs1.hubspotusercontent-eu1.net/hubfs/25513287/Marine%20System%20225.pdf?utm_medium=email&_hsenc=p2ANqtz-9pC6kqSzKbWgRmkgqG9j-wYCOMF1d8PxKQhSUoVjmWzAyNtmMafkUH_FqPBux0ihSNWLBkkrBgLtSHMuYBw4ubZRuzm_Tl9y2mT1MZxr3EZn6ovcY&_hsmi=88671217&utm_content=88671217&utm_source=hs_automation

Rijksoverheid. (2022). *Strategie IenW klimaat- en energieneutraal in 2030* [Retrieved July 26, 2025]. https://magazines.rijksoverheid.nl/ienw/duurzaamheidsverslag/2022/01/strategie-ienw-klimaat-en-energieneutraal-in-2030#:~:text=Het%20ministerie%20van%20Infrastructuur%20en,te%20wekken%20als%20we%20verbruiken.

ScandiNAOS AB. (n.d.). *MD97 Methanol Engines* [Retrieved July 13, 2025]. https://www.scandinaos.com/products.html#heading_MD97_methanol_engines

Schmaltz, T., Hartmann, F., Wicke, T., Weymann, L., Neef, C., & Janek, J. (2023). A roadmap for solid-state batteries. *Advanded Energy Materials*, *13(43)*, 2301886. https://doi.org/https://doi.org/10.1002/aenm.202301886

SKAO. (2020). *Handboek CO_2-prestatieladder 3.1* [Retrieved on August 2, 2024]. https://co2-prestatieladder.ams3.digitaloceanspaces.com/media/2020/documenten%202020/Prestatieladder%20Handboek%203.1_22-6-2020.pdf

Stark, C., Xu, Y., Zhang, M., Yuan, Z., Tao, L., & Shi, W. (2022). Study on applicability of energy-saving devices to hydrogen fuel cell-powered ships. *Journal of Marine Science and Engineering*, *10*(3). https://doi.org/10.3390/jmse10030388

Tesvolt Ocean. (n.d.-a). *Kaptein NMC Specifications Sheet* [Retrieved July 16, 2025]. https://www.tesvolt-ocean.com/_media/Produkte/Naviagtor/Kaptein_NMC_Navigator_Specifications_Sheet-v.C01.pdf

Tesvolt Ocean. (n.d.-b). *Kaptein NMC specifications sheet* [Retrieved March 10, 2025]. https://www.tesvolt-ocean.com/_media/Produkte/Kaptein/Kaptein_NMC_Navigator_Specifications_Sheet-v.C01.pdf

The Engineering Handbook. (2024). *Ship Power Prediction - Holtrop and Mennen*. https://enghandbook.com/calculators/power-prediction-holtrop-and-mennen/

The Engineering Toolbox. (2004). *Metals and Alloys - Densities* [Retrieved July 25, 2025]. https://www.engineeringtoolbox.com/metal-alloys-densities-d_50.html

Thyssenkrupp. (2023). *Density of Aluminium* [Retrieved July 17, 2025]. https://www.thyssenkrupp-materials.co.uk/density-of-aluminium.html

TNO. (n.d.). 15 dingen die je moet weten over waterstof [Retrieved on Oktober 8, 2024]. https://www.tno.nl/nl/duurzaam/co2-neutrale-industrie/schone-waterstofproductie/15-dingen-die-je-moet-weten-waterstof/

Van den Meer, I. (2023). *MAN hydrogen ICE engine* [Retrieved July 20, 2025]. https://iepieleaks.nl/man-hydrogen-ice-engine/

Van Hoecke, L., Laffineur, L., Campe, R., Perreault, P., Verbruggen, S. W., & Lenaerts, S. (2021). Challenges in the use of hydrogen for maritime applications. *Energy Environ. Sci.*, *14*, 815–843. https://doi.org/10.1039/D0EE01545H

Vervoordeldonk, S. (2025). *Predicting a nominal wake field* (tech. rep.). Delft University of Technology. https://resolver.tudelft.nl/uuid:4d6da853-6b50-4e32-8bae-29c7e4b53828

VPRO Tegenlicht. (2024, April). *De schaduwkant van de energietransitie en digitalisering | vpro tegenlicht* [Video. (Youtube)]. https://www.youtube.com/watch?v=vpiXdEsOmWE

Wissner, N., Healy, S., Cames, M., & Sutter, J. (2023). *Methanol as a marine fuel* (tech. rep.). Naturschutzbund Deutschland e.V. NABU. https://www.oeko.de/fileadmin/oekodoc/Methanol-as-a-marine-fuel.pdf

WRI, WBCSD. (2011). *Corporate Value Chain (Scope 3) Accounting and Reporting Standard*. https://ghgprotocol.org/sites/default/files/standards/Corporate-Value-Chain-Accounting-Reporing-Standard_041613_2.pdf

Wu, D., & Wu, F. (2023). Toward better batteries: Solid-state battery roadmap 2035+. *eTransportation*, *16*, 100224. https://doi.org/https://doi.org/10.1016/j.etran.2022.100224

Yu, X., Chen, R., Gan, L., Li, H., & Chen, L. (2023). Battery safety: From lithium-ion to solid-state batteries. *Engineering*, *21, 9-14*. https://doi.org/10.1016/j.eng.2022.06.022

Yuan, Y., Wang, J., Yan, X., Shen, B., & Long, T. (2020). A review of multi-energy hybrid power system for ships. *Renewable and Sustainable Energy Reviews*, *132*, 110081. https://doi.org/10.1016/j.rser.2020.110081

Yun, L., & Bliault, A. (2012). Hydrofoil craft. In *High performance marine vessels* (pp. 161–202). Springer US, Boston, MA. https://doi.org/10.1007/978-1-4614-0869-7_5

Zekalabs. (n.d.). *RedPrime 200kW, 1200V, 250A DC-DC Converter* [Retrieved July 16, 2025]. https://zekalabs.com/products/non-isolated-high-power-converters/dc-dc-converter-200kw-1200v/

zepp.solutions. (n.d.). *zepp.X150* [Retrieved April 11, 2025]. https://zepp.solutions/en/x150/

ZF. (n.d.). *Product selection guide 2025* [Retrieved July 19, 2025]. https://www.zf.com/products/media/industrial/marine/brochures_1/Product_Selection_Guide.pdf

Zincir, B., & Deniz, C. (2021). Methanol as a fuel for marine diesel engines. In P. C. Shukla, G. Belgiorno, G. Di Blasio, & A. K. Agarwal (Eds.), *Alcohol as an alternative fuel for internal combustion engines* (pp. 45–85). Springer Singapore. https://doi.org/10.1007/978-981-16-0931-2_4

A

Initial general energy storage requirements

In chapter 4, the calculation for the total required energy storage capacity for all 5 energy configurations is explained. The initial results of this calculation are presented in table A.1. The orange, blue and green colours respectively represent regions of type I, type II and type III. In this calculation, r_{batt} is chosen as 10%, as shown in the top row. If the power plant weight in that scenario is too high to converge without drastic dimension changes, than by extension that hybrid is also not feasible for any other value of r_{batt}.

Table A.1: General requirements for a battery-PEMFC electric hybrid energy storage based on the extreme operational scenarios

Energy specifications	Battery only		Primary battery - Secondary H2				H2 ICE		Methanol only		Primary methanol - Secondary battery			
			H2 PEMFC	*90%*	*Battery pack*	*10%*					*Battery pack*	*10%*	*Methanol*	*90%*
Time between bunkers	0.333	days	2	days	0.333	days	2	days	2	days	0.333	days	2	days
Installed power	909	kW	818	kW	541	kW	909	kW	909	kW	541	kW	818	kW
Battery extremes correction	30%				30%						30%			
Fuel margin	10%		10%		10%		10%		10%		10%		10%	
Required output energy	3430	kWh	14553	kWh	343	kWh	16170	kWh	16170	kWh	343	kWh	14553	kWh
Energy efficiency (storage to shaft)	64%		48%		64%		39%		37%		64%		37%	
Total required energy storage	**5384**	**kWh**	**30154**	**kWh**	**538**	**kWh**	**41082**	**kWh**	**43761**	**kWh**	**538**	**kWh**	**39385**	**kWh**
Number of units	230	batteries	6	cells	23	batteries					23	batteries		
Max time at surveillance speed	17.2	h	74.9	h			81.26	h	81.26	h	74.9	h		
Max time at increased speed	7.1	h	30.7	h			33.3	h	33.3	h	30.7	h		
Max time at full speed	3.8	h	3.8	h			17.79	h	17.79	h	3.8	h		
Time between bunkers	0.333	days	2	days	0.333	days	2	days	2	days	0.333	days	2	days
Installed power	1183	kW	1065	kW	940	kW	890	kW	890	kW	940	kW	1065	kW
Battery time step correction	30%				30%						30%			
Fuel margin	10%		10%		10%		10%		10%		10%		10%	
Required effective energy	5858	kWh	24855	kWh	586	kWh	27617	kWh	27617	kWh	586	kWh	24855	kWh
Energy efficiency (storage to shaft)	64%		48%		64%		39%		37%		64%		37%	
Total required energy storage	**9195**	**kWh**	**51500**	**kWh**	**920**	**kWh**	**70165**	**kWh**	**74740**	**kWh**	**920**	**kWh**	**67266**	**kWh**
Number of units	392	batteries	8	cells	40	batteries					40	batteries		
Max time at surveillance speed	23.6	h	102.6	h			111.36	h	111.36	h	102.6	h		
Max time at increased speed	8.0	h	34.9	h			37.8	h	37.8	h	34.9	h		
Max time at full speed	5.0	h	5.0	h			23.34	h	23.34	h	4.95	h		
Time between bunkers	0.333	days	2	days	0.333	days	2	days	2	days	0.333	days	2	days
Installed power	588	kW	529	kW	212	kW	890	kW	890	kW	212	kW	529	kW
Battery time step correction	40%				40%						40%			
Fuel margin	10%		10%		10%		10%		10%		10%		10%	
Required effective energy	1244	kWh	4924	kWh	124	kWh	5471	kWh	5471	kWh	124	kWh	4924	kWh
Energy efficiency (storage to shaft)	64%		48%		64%		39%		37%		64%		37%	
Total required energy storage	**1952**	**kWh**	**10203**	**kWh**	**195**	**kWh**	**13901**	**kWh**	**14807**	**kWh**	**195**	**kWh**	**13327**	**kWh**
Number of units	84	batteries	4	cells	9	batteries					9	batteries		
Max time at surveillance speed	19.7	h	80.1	h			86.85	h	86.85	h	80.1	h		
Max time at increased speed	8.6	h	35.1	h			38.0	h	38.0	h	35.1	h		
Max time at full speed	2.1	h	2.1	h			9.31	h	9.31	h	2.11	h		

B

Exposition of power plant weight & size calculation

In table B.1, estimations of the individual element weights and sizes are presented a vessel operating in a type I region. In table B.2, estimations of the individual element weights and sizes are presented a vessel operating in a type II region. In table B.3, estimations of the individual element weights and sizes are presented a vessel operating in a type III region.

Table B.1: Exposition of the estimated weights and sizes of the individual elements that are used to predict m_{PP} and V_{PP} of a vessel operating in a region of type I.

	Weight & size of energy storage and power equipment									
Energy storage & power equipment	**Battery electric**		**Battery-PEMFC hybrid**		**H2 ICE**		**Methanol ICE**		**Battery-methanol ICE hybrid**	
	weight (kg)	size (l)	weight (kg)	size (l)	weight (kg)	size (l)	weight (kg)	size (l)	weight (kg)	size (l)
Battery storage	25300	16445	2530	1644					2530	1644
Methanol storage							8109	10021	7318	5182
Hydrogen storage (on deck)			12036	53762	16427	73373				
Internal combustion engine					3128	3880	2502	3880	2502	3880
SCR+DPF					1136	4654	1136	4654	1023	4189
Fuel cells			2130	3570						
H2 distribution			420		420					
Fuel cell converters			180	245						
Battery converters	150	204	30	41	30	41	30	41	90	123
Electromotors	1360	743	1360	743					840	115
Electrical distribution components	1560	3272	1560	3272					1560	4891
Insulation	611		529						224	
Nitrogen generation							437	720	437	720
Cooling system	1464	4292	1464	4292	1464	4292	1464	4292	1464	4292
Batteries for hotel load					220	143	220	143		
Gearbox	511	503	511	503	511	503	511	503	511	503
Lubricants					200	160	200	160	200	160
Total weight & size (in t and m3)	**31.0**	**25.5**	**22.8**	**68.1**	**23.5**	**87.0**	**14.6**	**24.4**	**18.7**	**25.7**

Table B.2: Exposition of the estimated weights and sizes of the individual elements that are used to predict m_{PP} and V_{PP} of a vessel operating in a region of type II.

	Weight & size of energy storage and power equipment									
Energy storage & power equipment	**Battery electric**		**Battery-PEMFC hybrid**		**H2 ICE**		**Methanol ICE**		**Battery-methanol ICE hybrid**	
	weight (kg)	size (l)	weight (kg)	size (l)	weight (kg)	size (l)	weight (kg)	size (l)	weight (kg)	size (l)
Battery storage	43120	28027	4400	2860					4400	2860
Methanol storage							13713	17115	12361	8851
Hydrogen storage (on deck)			20590	91970	28009	125107				
Internal combustion engine					3128	3880	2502	3880	2502	3880
SCR+DPF					1479	6057	1479	6057	1331	5451
Fuel cells			2840	4760						
H2 distribution			420		420					
Fuel cell converters			240	327						
Battery converters	180	245	30	41	30	41	30	41	150	204
Electromotors	1900	920	1900	920					840	115
Electrical distribution components	2030	4259	2030	4259					2030	7217
Insulation	868		529						224	
Nitrogen generation							437	720	437	720
Cooling system	1906	5586	1906	5586	1906	5586	1906	5586	1906	5586
Batteries for hotel load					220	143	220	143		
Gearbox	511	503	511	503	511	503	511	503	511	503
Lubricants					200	160	200	160	200	160
Total weight & size (in t and m3)	**50.5**	**39.5**	**35.4**	**111.2**	**35.9**	**141.5**	**21.0**	**34.2**	**26.9**	**35.5**

Table B.3: Exposition of the estimated weights and sizes of the individual elements that are used to predict m_{PP} and V_{PP} of a vessel operating in a region of type III.

	Weight & size of energy storage and power equipment									
Energy storage & power equipment	**Battery electric**		**Battery-PEMFC hybrid**		**H2 ICE**		**Methanol ICE**		**Battery-methanol ICE hybrid**	
	weight (kg)	size (l)	weight (kg)	size (l)	weight (kg)	size (l)	weight (kg)	size (l)	weight (kg)	size (l)
Battery storage	9240	6006	990	643					990	643
Methanol storage							2871	3391	2603	1753
Hydrogen storage (on deck)			4088	18259	5602	25021				
Internal combustion engine					3128	3880	2502	3880	2502	3880
SCR+DPF					735	3011	735	3011	662	2710
Fuel cells			1420	2380						
H2 distribution			420		420					
Fuel cell converters			120	163						
Battery converters	90	123	30	41	30	41	30	41	60	82
Electromotors	980	502	980	502					840	115
Electrical distribution components	1009	2117	1009	2117					1009	2667
Insulation	288		417						224	
Nitrogen generation							437	720	437	720
Cooling system	947	2777	947	2777	947	2777	947	2777	947	2777
Batteries for hotel load					220	143	220	143		
Gearbox	511	503	511	503	511	503	511	503	511	503
Lubricants					200	160	200	160	200	160
Total weight & size (in t and m3)	**13.1**	**12.0**	**10.9**	**27.4**	**11.8**	**35.5**	**8.5**	**14.6**	**11.0**	**16.0**

C

Reference models for power plant elements

For the estimation of the weight of the ICEs, a series of MAN diesel engines is used as a reference. As reported by MAN Engines, these engines are designed for typical applications like ambulance and police boats, pilot boats, passenger boats and seagoing patrol boats (MAN Rollo, n.d.).

Table C.1: Series of diesel engines used as a reference for the estimation of the hydrogen and methanol engines

ICE model	Power (kW)	Weight (kg)	L (dm)	B (dm)	H (dm)	Volume (l)
D2676 - LE 446	537	1251	18.0	9.9	11.0	1940
D2676 - LE 426	588	1251	18.0	9.9	11.0	1940
D2676 - LE 456	625	1251	18.0	9.9	11.0	1940
D2868 - LE 426	735	1780	17.5	11.5	11.8	2368
D2868 - LE 453	824	1941	17.5	11.5	12.2	2459
D2868 - LE 436	882	1941	17.4	11.5	12.2	2446
D2868 - LE 466	956	1941	17.4	11.5	12.2	2446
D2862 - LE 446	1029	2270	21.3	11.5	12.3	3021
D2862 - LE 426	1140	2270	21.3	11.5	12.3	3021
D2862 - LE 456	1213	2420	21.4	11.5	12.7	3137

In case the vessel is electrically driven, an electric motors is needed. In table C.2, the selection of motors that are considered for the emissionless design is shown.

Table C.2: Overview of the considered electric motors

Electromotor	Producer	Cont. power (kW)	Cont. torque (Nm)	Weight (kg)	L (dm)	B (dm)	H (dm)	Volume (l)	Cont. RPM	Motor type	Note
EM-PMI375-T200-690V [1]	Danfoss	44	157	98	2.78	4.5	4.5	56.30	2700	Radial flux	
EM-PMI375-T200 [1]	Danfoss	56	189	98	2.78	4.5	4.5	56.30	2600	Radial flux	
EM-PMI300-T310 [1]	Danfoss	65	389	125	3.77	4.08	4.08	62.76	1600	Radial flux	
EM-PMI375-T500 [1]	Danfoss	78	575	172	3.68	4.5	4.5	74.52	1300	Radial flux	
EM-PMI375-T500-690V [1]	Danfoss	88	444	172	3.68	4.5	4.5	74.52	1900	Radial flux	
EM-PMI240-T180 [1]	Danfoss	108	117	85	3.17	3.05	3.05	29.49	8800	Radial flux	
EM-PMI375-T800-690V [1]	Danfoss	138	659	210	4.28	4.5	4.5	86.67	2000	Radial flux	
EM-PMI375-T800 [1]	Danfoss	170	854	210	4.28	4.5	4.5	86.67	1900	Radial flux	
EM-PMI375-T1100-690V [1]	Danfoss	180	1076	295	5.48	4.5	4.5	110.97	1600	Radial flux	
EM-PMI375-T1100 [1]	Danfoss	231	1225	295	5.48	4.5	4.5	110.97	1800	Radial flux	
EM-PMI540-T1500 [1]	Danfoss	278	1662	390	5.31	6.48	6.48	222.97	1600	Radial flux	
EM-PMI540-T2000 [1]	Danfoss	405	2276	490	5.98	6.48	6.48	251.10	1700	Radial flux	
EM-PMI540-T3000 [1]	Danfoss	470	2991	680	8.4	6.65	6.65	371.47	1500	Radial flux	
EM-PMI540-T4000-1200 [1]	Danfoss	590	4692	950	10.4	6.65	6.65	459.91	1200	Radial flux	
EM-PMI540-T4000 [1]	Danfoss	777	4639	950	10.4	6.65	6.65	459.91	1600	Radial flux	
Emrax 348 [2]	Emrax	140	425	43.9	1.07	3.48	3.48	12.96	3250	Axial flux	Double stackable
PH.382 [3]	Phi-power	180	550	83	2.3	3.8	3.8	33.21	3500	Axial flux	Triple stackable
AXM4 [4]	Beyond	230	600	48	1.85	4.25	4.79	37.66	3600	Axial flux	Triple stackable
D1700 [5]	Evolito	250	1500	40	1.7	4.5	4.5	34.43	1600	Axial flux	Primarily for aviation

[1](Danfoss, n.d.)
[2](Emrax, n.d.)
[3](Phi-power AG, n.d.)
[4](Beyond Motors, n.d.)
[5](Evolito, n.d.)